

Inferring regulators of cell identity in the human adult pancreas

Lotte Vanheer^{1,†}, Federica Fantuzzi^{2,†}, San Kit To¹, Andrea Schiavo², Matthias Van Haele³, Tessa Ostyn³, Tine Haesen¹, Xiaoyan Yi², Adrian Janiszewski¹, Joel Chappell¹, Adrien Rihoux¹, Toshiaki Sawatani², Tania Roskams³, Francois Pattou^{4,5,6}, Julie Kerr-Conte^{4,5,6}, Miriam Cnop^{2,7,*} and Vincent Pasque^{1,*‡}

¹Department of Development and Regeneration; KU Leuven - University of Leuven; Single-cell Omics Institute and Leuven Stem Cell Institute, Herestraat 49, B-3000 Leuven, Belgium, ²ULB Center for Diabetes Research; Université Libre de Bruxelles; Route de Lennik 808, B-1070 Brussels, Belgium, ³Department of Imaging and Pathology; Translational Cell and Tissue Research, KU Leuven and University Hospitals Leuven; Herestraat 49, B-3000 Leuven, Belgium, ⁴University of Lille, Inserm, CHU Lille, Institute Pasteur Lille, U1190-EGID, F-59000 Lille, France, ⁵European Genomic Institute for Diabetes, F-59000 Lille, France, ⁶University of Lille, F-59000 Lille, France and ⁷Division of Endocrinology; Erasmus Hospital, Université Libre de Bruxelles; Route de Lennik 808, B-1070 Brussels, Belgium

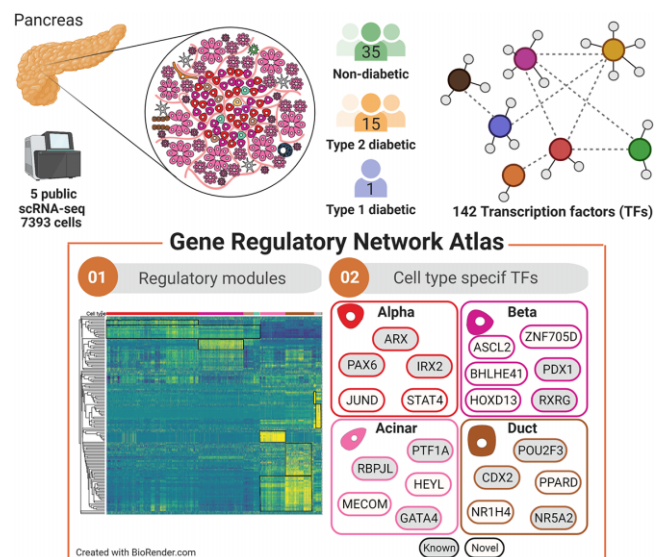
Received December 20, 2022; Revised June 17, 2023; Editorial Decision June 20, 2023; Accepted June 28, 2023

ABSTRACT

Cellular identity during development is under the control of transcription factors that form gene regulatory networks. However, the transcription factors and gene regulatory networks underlying cellular identity in the human adult pancreas remain largely unexplored. Here, we integrate multiple single-cell RNA-sequencing datasets of the human adult pancreas, totaling 7393 cells, and comprehensively reconstruct gene regulatory networks. We show that a network of 142 transcription factors forms distinct regulatory modules that characterize pancreatic cell types. We present evidence that our approach identifies regulators of cell identity and cell states in the human adult pancreas. We predict that HEYL, BHLHE41 and JUND are active in acinar, beta and alpha cells, respectively, and show that these proteins are present in the human adult pancreas as well as in human induced pluripotent stem cell (hiPSC)-derived islet cells. Using single-cell transcriptomics, we found that JUND represses beta cell genes in hiPSC-alpha cells. BHLHE41 depletion induced apoptosis in primary pancreatic islets. The comprehensive gene regulatory network atlas can be explored interactively online. We anticipate our analysis to be the starting point for a more sophisticated dissection of how tran-

scription factors regulate cell identity and cell states in the human adult pancreas.

GRAPHICAL ABSTRACT



INTRODUCTION

A fundamental question in biology is how a single genome gives rise to the great diversity of cell types that make up organs and tissues. A key goal is to map all cell types

*To whom correspondence should be addressed. Tel: +32 16 376283; Fax: +32 16 330827; Email: vincent.pasque@kuleuven.be
Correspondence may also be addressed to Miriam Cnop. Tel: +32 2 555 6305; Fax: +32 2 555 6239; Email: miriam.cnop@ulb.be

†The authors wish it to be known that, in their opinion, the first two authors should be regarded as Joint First Authors.

‡Lead contact.

of developing and mature organs such as the pancreas, an essential organ at the basis of multiple human disorders including diabetes and cancer (1–3). Single-cell RNA-sequencing (scRNA-seq) provides a powerful tool to resolve cellular heterogeneity, identify cell types and capture high-resolution snapshots of gene expression in individual cells (4). With the advent of single-cell transcriptomics, great progress has been made toward the creation of a reference cell atlas of the pancreas (3,5–14). Work from several groups provided cellular atlases of the pancreas during mouse development (15–18), in adult mice (19) and in human fetal (20–25) and adult pancreas (3,5–10,19,26–28). Efforts have also been made to map cellular identity during pancreas development starting from human pluripotent stem cells (11,22,27,29–38). Taken together, these studies provide an opportunity to better understand the establishment and maintenance of cellular identity among different pancreatic cell types.

Work over the past decades indicated that cellular identity is established by combinations of transcription factors (TFs) that recognize and interact with *cis*-regulatory elements in the genome (39). TFs, together with chromatin modifiers, deploy gene expression programs. A small number of core TFs are thought to be sufficient for the establishment and maintenance of gene expression programs that define cellular identity during and after development (40). Studies conducted in both mouse and human have successfully identified TFs that are pivotal for the acquisition and maintenance of pancreatic cell fates (41). These include PDX1 (42,43), MAFA (44), NGN3 (45), NKX2.2 (46), PAX4 (47), NKX6.1, NEUROD1 (48), ARX (49), MAFB (50), RFX6 (51,52), GATA4 (53), FOXA2 (54) and SOX9 (43,55). Conditional deletion of TFs such as FOXA2 and PDX1 in adult beta cells results in the loss of cellular identity and function (56,57). Robust genetic evidence for the role of these TFs in establishing human pancreatic cell identity is provided by the identification of TF loss-of-function mutations that cause pancreatic agenesis (15,58–61) or neonatal or young-onset diabetes (60,62–66). In addition, TF overexpression can reprogram somatic cells to adopt alternative identities (67–69). For example, the induced expression of *Ngn3*, *Pdx1* and *Mafa* was shown to reprogram mouse alpha cells into beta-like cells *in vivo* (42). However, how key TFs underlie the maintenance of cellular identity in the human pancreas remains incompletely understood.

Multiple approaches to reconstruct gene regulatory networks (GRNs) from bulk and single-cell omics data have been developed (39,70–72). In particular, it is now possible to combine single-cell transcriptomic data with either *cis*-regulatory information (73–76) or chromatin accessibility (74,75) to infer GRNs. Because TFs recognize DNA motifs in the genome, one can measure if inferred target genes are expressed within single cells, and therefore quantify the activity of TFs. Such approaches have revealed the regulatory programs in distinct systems including the *Drosophila* brain (76), cancer (77), during early mouse embryonic (78) and pancreas development (79), reprogramming to induced pluripotency (80), in a mouse cell atlas (81) and a human cell atlas (3).

Analysis of GRNs in the human adult pancreas has identified distinct endocrine and exocrine regulatory states with

multiple stable cell states for alpha, beta and ductal cells (82). No change in GRN activity of alpha and beta cells was reported in type 2 diabetes or related to body mass index (BMI) (82). Previous data show that type 2 diabetic (83–86) and non-diabetic human islet preparations vary greatly depending on age (9,87) and BMI (88) warranting the exploration of GRNs across multiple integrated datasets. Hence, it remains unclear whether previous GRN findings can be extrapolated to a broader, highly heterogeneous population comprising non-diabetic and type 2 diabetic donors. The development of integration methods provides an opportunity to analyze multiple scRNA-seq studies from multiple laboratories and patients (89,90). Additional knowledge on how GRNs maintain cellular identity in the human adult pancreas may further the understanding of disease states and improve ongoing efforts to convert human induced pluripotent stem cells (hiPSCs) into functional, mature beta cells for diabetes treatment.

Here, we build an integrated human pancreas gene regulatory atlas. In this resource, we use single-cell transcriptomes of the human adult pancreas, taking advantage of integration strategies and computational tools to reconstruct GRNs. Our analysis identifies the GRN landscape and candidate regulators that may regulate cellular identity and cell states in the human adult pancreas. Finally, we knockdown candidate TFs in primary and hiPSC-derived islets to test their implication in regulating pancreatic GRNs.

MATERIALS AND METHODS

Reagents

See Table 1.

Biological resources

See Table 2.

Data availability/sequence data resources

See Table 3.

Web sites/data base referencing

See Table 4.

Statistical analyses

Statistical tests were performed using the stats package (v3.5.2) in R and GraphPad Prism 9 (GraphPad Software). Wilcoxon rank sum tests with FDR correction were used as indicated. All data, unless indicated otherwise, are presented as the mean \pm s.d. *P* values of <0.05 were considered statistically significant.

Method details

Motif discovery of bulk ATAC-seq data. Paired-end raw reads for bulk ATAC-seq (see Data Availability/Sequence Data Resources) were downloaded from SRA using SRA toolkit (v2.9.4). Reads were aligned and further analyzed

Table 1. Reagents

Reagent	Catalog number	Identifier
Monoclonal mouse anti-human ASCL2	Cat# MAB4418, clone 7E2	Millipore, RRID:AB_10561764
Rabbit anti-human JUN	Cat# HPA063029	Atlas Antibodies, RRID:AB_2684925
Rabbit anti-human HEYL	Cat# HPA076960	Atlas Antibodies, RRID:AB_2732326
Rabbit anti-human BHLHE41	Cat# HPA056035	Sigma Aldrich, RRID:AB_2683017
Guinea pig anti-human INS	Cat# IR002	Agilent, RRID:AB_2800361
Monoclonal mouse anti-human GCG	Cat# G2654	Sigma-Aldrich, RRID:AB_259852
Goat Anti-Guinea Pig IgG Alexa Fluor 568	Cat# A-11075	Thermo Fisher Scientific, RRID:AB_2534119
Donkey anti-Rabbit IgG Alexa Fluor 488	Cat# A-21206	Thermo Fisher Scientific, RRID:AB_2535792
Donkey Anti-Mouse IgG Alexa Fluor 647	Cat# A-31571	Thermo Fisher Scientific, RRID:AB_162542
RNeasy Micro Kit	Cat#74004	Qiagen
Platinum™, SYBR™ Platinum™ SYBR™ Green qPCR SuperMix-UDG	Cat# 11733046.00	Thermo Fisher Scientific

Table 2. Biological resources

Resource	Origin
Control iPSC line HEL115.6	(95)
Control iPSC line 1023A	(96)
Human pancreas sections	Biobank of the University Hospital Leuven (Leuven, Belgium)
Non-diabetic human pancreatic islets	Laboratory for Translational Research on Diabetes (Lille, France)
Type 2 diabetic human pancreatic islets	Laboratory for Translational Research on Diabetes (Lille, France)

using the ENCODE ATAC-seq pipeline with default parameters using the ENCODE human reference genome GRCh38.15 (Lee, 2016). Bed files containing the global open chromatin landscape of adult alpha (Alpha_1; EA4 and Alpha_2; EA28), beta (Beta_1; EA5 and Beta_2; EA29), acinar (Acinar_1; EA7 and Acinar_2; EA27) and ductal (EA11) cells or cell type specific differentially accessible regions were used as input for motif discovery by HOMER (v4.10.4) using the ‘findMotifsGenome.pl’ with options using hg38 with size given (Heinz *et al.*, 2010). The TFs whose motifs identified by HOMER correspond with TFs identified by pySCENIC are visualized in Supplementary Figure S2A.

Analysis of publicly available scATAC-seq data. Motif discovery results by HOMER of a publicly available scATAC-seq dataset (see Key Resource Table) was retrieved from Supplementary Table S8 of (Rai *et al.* 2020). The TFs whose motifs identified by HOMER correspond with TFs identified by pySCENIC are visualized in Supplementary Figure S2B using pheatmap (v1.0.12).

Analysis of publicly available scRNA-seq data. Raw reads for five publicly available scRNA-seq datasets (see Key Resource Table) were downloaded from SRA using SRA toolkit (v2.9.4). Afterwards, reads were aligned to the human reference genome GRCh38.95 using STAR (v2.5.3a) with default parameters followed by the conversion to the coordinate sorted BAM format. Next, the featureCounts command from the ‘Rsubread’ (v1.5.2) package in R (v3.6.1) was used to assign mapped reads to genomic features. Low quality transcriptomes with a mitochondrial contamination greater than 5% and less than 200 expressed

genes per cell were excluded from subsequent analyses. The resulting raw count matrix was batch corrected using the FindIntegrationAnchors and IntegrateData functions from the ‘Seurat’ package (v3.1.1) after which subsequent analyses were carried out in the R package ‘Seurat’ (v3.1.4). Gene expression was used to cluster all 7393 cells with uniform manifold approximation and projection (UMAP), using Seurat’s function RunUMAP.

Clusters for cell type annotation were defined using Seurat’s shared nearest neighbor algorithm FindClusters function after which differential expression analysis was performed using Wilcoxon’s rank sum test with a minimum cut-off of 0.25 average log fold change and min.pct of 0.25.

pySCENIC. GRNs were inferred using pySCENIC (python implementation of SCENIC, v0.9.15) in Python version 3.6.9 (91). Integrated read counts were used as input to run GENIE3 (92) which is part of arboreto (v0.1.5). GRNs were subsequently inferred using pySCENIC with the hg38_refseq-r80 motif database and default settings. To control for the stochasticity, which is inherent to pySCENIC, a consensus GRN was generated by merging results from five repeat pySCENIC runs. If regulons were identified in multiple pySCENIC runs, only the regulon with the highest AUC value was retained. Regulon activity represented by AUCell values was used to cluster all 7393 cells with UMAP, using Seurat’s RunUMAP function.

All 142 regulons within non-diabetic cell types were visualized using the ‘clustermap’ function of the Python package ‘seaborn’ (v0.9.0). The z-score for each regulon across all cells was calculated using the z-score parameter of the seaborn ‘clustermap’ function.

Extended analysis of the target genes of specific regulons was conducted in Cytoscape (v3.7.1) using the iRegulon application (v1.3). The list of target genes of a specific regulon was downloaded from the loom file through the SCoPe platform (<https://github.com/pasquelab/scPancreasAtlas>) (76).

Regulon ranking. To quantify the cell-type specificity of a regulon, we utilized an entropy-based strategy as described previously (Suo *et al.*, 2018) using the AUCell matrix as input in MATLAB R2019b. The top 10 most specific regulons were subsequently visualized using the R package ggplot2

Table 3. Data availability/sequence data resources

Resource	Reference	Repository	Identifier
Reanalyzed human pancreatic scRNA-seq dataset	(10)	GEO	GEO: GSE86469
Reanalyzed human pancreatic scRNA-seq dataset	(8)	GEO	GEO: GSE81608
Reanalyzed human pancreatic scRNA-seq dataset	(7)	GEO	GEO: GSE83139
Reanalyzed human pancreatic scRNA-seq dataset	(9)	GEO	GEO: GSE81547
Reanalyzed human pancreatic scRNA-seq dataset	(6)	ArrayExpress	ArrayExpress: E-MTAB-5061
Reanalyzed human pancreatic bulk ATAC-seq dataset of FACS sorted beta, alpha, ductal and acinar cell populations	(113)	GEO	GEO: GSE79468
Human pancreatic scATAC-seq dataset	(114)	Publication	Supplementary Table S8
.loom file containing regulon and gene expression data	This study	GEO	GEO: GSE156490
Human Pancreas Analysis Program Database		https://hmap.pmacs.upenn.edu	HPAP-RRID:SCR_016202
scRNA-seq of siRNA treated hiPSC-derived islet cells	This study	GEO	GEO: GSE218547

Table 4. Web sites/data base referencing

Software	Version	Identifier
SRA toolkit	v2.9.4	
STAR	v2.5.3a	RRRID:SCR_015899
Rsubread	v1.5.2	RRRID:SCR_016945
ENCODE ATAC-seq pipeline		(Lee, 2016)
HOMER	v4.10.4	RRRID:SCR_010881
pheatmap	v1.0.12	RRRID:SCR_016418
Integrative Genomics Viewer	V2.8.0	RRRID:SCR_011793
Seurat	v3.1.1	RRRID:SCR_007322
seaborn	v0.9.0	RRRID:SCR_018132
pySCENIC	v0.9.15	RRRID:SCR_017247
Cytoscape	v3.7.1	RRRID:SCR_003032
iRegulon (Cytoscape plugin)	v1.3	(Janky <i>et al.</i> , 2014)
MATLAB	R2019b	RRRID:SCR_001622
GraphPad Prism	9	RRRID:SCR_002798
ggpubr	v0.2.5	RRRID:SCR_021139
ggplot2	v3.1.1	RRRID:SCR_014601
LoomPy	v2.0.17	RRRID:SCR_016666
R	v3.6.1	RRRID:SCR_001905
Python	3.6.9	RRRID:SCR_008394

(v3.1.1). The complete regulon ranking list is available in Supplementary Table S1.

HPAP scRNA-seq data processing and analysis. Raw fastq files of scRNA-seq data were obtained from the portal of Human Pancreas Analysis Program (<https://hmap.pmacs.upenn.edu>). We analyzed 12 type 2 diabetic donors (HPAP-058, 088, 065, 051, 081, 083, 085, 057, 091, 079, 070, 061) and 32 non-diabetic donors (042, 044, 039, 047, 034, 038, 043, 024, 072, 050, 019, 029, 036, 026, 082, 045, 052, 049, 027, 056, 035, 037, 040, 059, 075, 022, 054, 074, 063, 077, 093, 053). Cell Ranger (10x Genomics; v6.1.2) was used for alignment (reference genome hg38) and filtering of sequencing reads. For each sample, decontamination of the ambient mRNA was done with SoupX (v1.6.1) by using the automatic selection of the background genes to adjust the gene profiles. The new single-cell gene expression profiles were imported into Seurat (v4.1.1) for quality control. We kept genes expressed in at least three cells that express at least 200 genes. Potential doublet cells were evaluated by R package scDbIFinder (v3.16) and removed. Further filtering was performed by criteria of nFeature_RNA <9000, percent of mitochondrial genes <10 and nCount_RNA <10 000. We obtained 78 927 single cells for downstream analysis.

We next used the Seurat SCTransform (SCT) function to measure the differences in sequencing depth per cell and normalize the counts by removing the variation due to sequencing depth (nUMIs). Top 3000 of the variable features were selected to perform dimensionality reduction by principal component analysis (PCA) and UMAP embedding. Lastly, R package scSorter (v0.0.2) was used to assign cells to known cell type based on the marker genes. We extracted the ‘alpha’, ‘beta’, ‘acinar’ and ‘ductal’ cells to check the top 10 regulons predicted by SCENIC analysis in the present study.

scRNA-seq sample preparation. hiPSC islets were washed with Versene (Thermo Fisher Scientific, 15040066) and incubated with Accutase (Sigma-Aldrich, A6964-100ML) for 10 min at 37°C. Dissociation was stopped by the addition of PBS supplemented with 1% bovine serum albumin (BSA). Dissociated cells were washed twice in PBS (1%BSA) buffer, centrifuged at 300 rcf for 5 min, filtered using Flowmi 40 µm tip strainer (Bel-Art, H13680-0040), counted and adjusted to 1×10^6 cells ml⁻¹ cells in PBS (1%BSA) for encapsulation. Cell count and viability were measured using the Luna-Fl automated Fluorescence Cell Counter (Logos Biosystems).

For each siRNA treatment, 6000 cells were loaded onto the 10x Chromium Single Cell Platform (10X Genomics) using the Next GEM Single Cell 3' library and Gel Bead Kit (v3.1 chemistry) according to manufacturer's instructions (10x User Guide CG000204, Revision D). RNA quality was assessed using TapeStation (Agilent). Libraries were quantified using TapeStation (Agilent), the Qubit 2.0 (ThermoFisher Scientific) and KAPA Library Quantification Kit for Illumina Platform (KAPA Biosystems) before pooling. Libraries were pooled in equimolar amounts for paired-end sequencing on an Illumina NextSeq 2000 instrument to yield ~168 million (range 147–195 million) 100-bp-long reads on average per sample.

scRNA-seq analysis. Raw data was processed using the 10x Genomics Cell Ranger software (v4.0.0) and mapped to the pre-built human reference genome GRCh38-2020-A. Contamination by background RNA from disrupted cells was estimated and corrected for using SoupX (93) with Seurat identified clusters, and known cell type specific marker genes (GCG, TTR; INS, IAPP; SST; PPY;

GHRL; CPA1, CLPS, CPA2, REG1A, CELA3A, CTRB1, CTRB2, PRSS2; KRT19, VTCN1). Cells with less than 200 expressed genes and more than 25% mitochondrial reads were excluded from future analyses. DoubletFinder (v2.0.3) (94) was used with default settings to identify and remove potential doublets. The resulting counts were normalized, scaled and analyzed for PCA and UMAP on the first 20 principle components (PCs) using 2000 variable genes using Seurat (v3.1.1). Clusters for cell type annotation were defined using Seurat's shared nearest neighbor algorithm as defined above.

To compare our dataset to the sc-derived and primary cell populations described in (35), we downloaded the count matrix and metadata files from the Single Cell Portal from the Broad Institute (SCP1526). The resulting Seurat object was integrated with our dataset using the FindIntegrationAnchors and IntegrateData functions from the 'Seurat' package (v3.1.1) after which subsequent analyses were carried out in the R package 'Seurat' (v3.1.4). Gene expression was used to cluster all 57158 cells with UMAP, using Seurat's function RunUMAP.

Human islets. Human islets (seven non-diabetic donors, age 43 ± 15 years, BMI 30 ± 6 kg/m² and one type 2 diabetic donor, age 66 years, BMI 36.5 kg/m²) were isolated by enzymatic digestion and density gradient purification in Lille or Edmonton, with the approval of the local Ethical Committee. After overnight recovery in Ham's F-10 containing 6.1 mM glucose, 10% FBS, 2 mM GlutaMAX, 0.75% BSA, 50 units/ml penicillin, and 50 µg/ml streptomycin, human islets were dispersed for RNA silencing. The percentage of beta cells, assessed by insulin immunofluorescence, was $50 \pm 11\%$ (mean \pm SD).

hiPSC-derived islet cell differentiation and immunocytochemistry. Control iPSC lines HEL115.6 (95) and 1023A (96) were differentiated into pancreatic islet cells using a previously published 7-step protocol (97,98). Briefly, iPSCs were cultured in Matrigel (Corning BV, #354277)-coated plates in E8 medium (Life Technology #A1517001). When cells reached 70–80% confluency, they were incubated with Accutase (3 min) in order to obtain a single cell solution. Cells were seeded at density 15.6 million cells/6-well plate in E8 medium supplemented with ROCK inhibitor (STEM CELLS Technologies #72304, 10 µM). Sixteen-to-twenty-four hours later E8 medium was refreshed and, when confluency was reached, cells were differentiated in Matrigel-coated plates until the stage of pancreatic progenitors (stage 4). At the end of this stage, cells were seeded into 24-well Aggrewell 400 microwell plates (Stem Cell Technologies) at a density of 0.9×10^6 cells per well after which differentiation was carried out as described previously until stage 7 (97). Overviews of the differentiation protocol and efficiency are shown in Supplementary Figure S4 and Supplementary Tables S2 and S3.

Stage 7 differentiated islet cells were washed twice with PBS containing 0.5 mM EDTA and incubated in Accumax (SIGMA #A7089) for 8 min at 37 °C after which 50% volume of KnockOut Serum Replacement (ThermoFisher #10828028) was added to stop the reaction. After centrifugation at 400 g for 5 min at room temperature, cells were re-

suspended in 1 ml HAM's F-10 medium, supplemented as indicated before (Demine *et al.*, 2020). 75000 cells in 500 µl medium were seeded per square of a Nunc Lab-Tek II ICC chamber (ThermoFisher).

Immunohistochemistry analyses were carried out largely as described previously (99), using the following primary antibodies: INS (Dako (Agilent), IR002, Ready to use solution), GCG (Sigma-Aldrich, G2654, 1/1000) and JUND (Atlas Antibodies, HPA063029, 1/100) and secondary antibodies A-11075, A-21206, A-31571 (ThermoFisher, 1/500). Pictures were taken using an Axiovert fluorescence microscope (Zeiss).

RNA silencing in dispersed human islets and hiPSC-derived islets. Dispersed human islets and hiPSC-derived islets were transfected with siRNAs for human JUND, (Dharmacon, LQ-003900–00-0002) or human BHLHE41 (Dharmacon, LQ-010043–00-0002). siRNA with no homology to any known mammalian gene was used as negative control (AllStars Negative Control siRNA, Qiagen). siRNA-Lipofectamine RNAiMAX (Invitrogen, Life Technologies) complexes were formed in Opti-MEM and diluted four times in Ham's F-10 medium without BSA or penicillin-streptomycin. Transfection was done using 30 nM siRNA and Lipofectamine at a final dilution of 1/250. Medium was refreshed after 16 hours and cells were studied after another 48 hours.

Assessment of cell apoptosis. The percentage of apoptotic cells was determined by nuclei staining with propidium iodide (5 µg/ml in PBS, Sigma-Aldrich) and Hoechst 33342 (10 µg/ml in PBS, Sigma-Aldrich), as described (96,100–104). This method (images available in (99)) has previously been validated against other methods to assess apoptosis, including electron microscopy (105,106), DNA strand breaks (100,101), Bax translocation (101), caspase cleavage (101,102) and cytochrome C release (103). A minimum of 500 cells were counted for each experiment by two operators, one of them unaware of sample identity. The proportion of apoptotic cells was calculated by quantifying propidium iodide-positive apoptotic nuclei relative to total cell number. The Pearson and Spearman correlation coefficient between apoptosis and BHLHE41 or JUND transcript levels was calculated using the R-package ggpubr (v0.2.5).

mRNA extraction and real time PCR. Total RNA was extracted using the RNeasy Plus micro kit (Qiagen), according to the manufacturer's instructions. Briefly, cells were washed once with PBS and collected in 100 µl of the kit's lysis buffer. RNA was eluted in 14 µl and retro-transcribed as described previously (107). Primer sequences are listed in Supplementary Table S4. All assays had an efficiency above 95%. Relative quantities of each transcript were calculated as arbitrary units from comparison to the standard curve. Relative expression level of the target transcript was presented as the ratio of the target transcript quantity to the reference transcript quantity (GAPDH, ACTB).

Immunohistochemistry. Briefly, 4 µm tissue sections were retrieved from 4% formalin-fixed, paraffin-embedded tissue blocks of normal pancreas tissue (68-year-old male, 59 year-old-male and 64-year-old female) from the biobank of the

University Hospital in Leuven (Belgium). Two pathologists (M.V.H. and T.R.) separately evaluated all histological sections. This study was approved by the ethical committee of the University Hospital in Leuven (Belgium) (S32980).

Immunohistochemistry analyses were carried out largely as described previously (108), using primary antibodies against the following proteins: ASCL2 (Merck, MAB4418, clone 7E2, 1/5000), JUND (Atlas Antibodies, HPA063029, 1/50), BHLHE41 (Sigma Aldrich, HPA056035, 1/25), HEYL (Atlas Antibodies, HPA076960, 1/200) and INS (Agilent, IR002, 1/100). Pictures were taken using a Leica DMLB (Leica Microsystems).

SCope. The integrated scRNA-seq data and pySCENIC results can be explored interactively in SCope (76). Loompy (v2.0.17) (Linnarsson Lab., 2015) was used to create the loom files which were uploaded to SCope. The embedding of the regulon and integrated gene expression based UMAP clustering, as seen in this article, were added to the loom file.

In vitro glucose-stimulated insulin secretion assay. Fifty aggregates were pre-incubated with Krebs buffer (Human Cell Design, #BK-25) supplemented with 0.1% BSA and 2.8 mM glucose for 90 min prior the sequential exposure to glucose 2.8 mM, 16.7 or 16.7 mM glucose plus 10 μ M forskolin. Each incubation lasted for 30 min and supernatants were collected for insulin measurement by ELISA (Merckodia, 10-1113-10). Intracellular insulin was extracted using acid ethanol (95% ethanol, 5% 12N hydrochloric acid) and quantified by human insulin ELISA. Data of insulin secretion and content were normalized to total protein content, measured by protein assay dye (Bio-Rad, #5000006).

RESULTS

Integrated analysis of scRNA-seq data identifies 12 human adult pancreatic cell types

Integrating multiple human adult pancreas scRNA-seq datasets can improve the power of scRNA-seq analyses to create a comprehensive human adult pancreas cell atlas. We set out to analyze and integrate five publicly available datasets covering a total of 35 non-diabetic, one type 1 diabetic and 15 type 2 diabetic individuals using Seurat v3.0 canonical correlation analysis (CCA) integration tools (Figure 1A, Supplementary Table S5) (6–10,109,110). After filtering out low quality transcriptomes and data integration, uniform manifold approximation and projection for dimension reduction (UMAP) visualization revealed that 7393 cells localized into distinct clusters (Figure 1B, Supplementary Figure S1A, B). Cells from each original dataset localized together suggesting that there is good correspondence between identical cell types from different datasets.

We next sought to identify pancreatic cell types (Figure 1C). Clustering analyses based on the expression of well-established cell type specific markers led to the identification of eight cell types in the human adult pancreas: beta, alpha, gamma, delta, acinar, ductal, stellate and endothelial cells (Figure 1D, Supplementary Table S6). UMAP visualization allowed the segregation of endocrine, exocrine and other lineages (Supplementary Figure S1C). Beta cells grouped together, away from other clusters and were marked by INS

(Figure 1E). Other distinct clusters corresponded to alpha, gamma and delta cells based on global transcriptional similarity and GCG, PPY and SST, and other markers, respectively (Figure 1E, Supplementary Table S6). Using a similar approach, we detected other, previously described, major pancreatic cell types including acinar, ductal, endothelial and stellate cells (Figure 1D, Supplementary Figure S1C, D). All cell types were detected in both non-diabetic and type 2 diabetic pancreases (Figure 1F). Four additional rare cell populations, that cannot be robustly identified through clustering analyses, were identified manually by assessing GHRL (epsilon cells), TPS1AB (mast cells), CD86 (Major histocompatibility complex (MHC) class 2 cells) and SOX10 (schwann cells) (Figure 1G) (6,111). These rare cell types often cluster with other common cell types. Importantly, our annotation largely recapitulated previous annotations (Supplementary Figure S1D–F). In summary, we reconstructed an integrated single-cell atlas of the human adult pancreas, and annotated 12 pancreatic cell types.

Reconstruction of gene regulatory networks in the human adult pancreas

Next, we set out to comprehensively reconstruct GRNs for all pancreatic cell types from single-cell transcriptomic data, applying single-cell regulatory network inference and clustering (pySCENIC) (112,91). PySCENIC links *cis*-regulatory sequence information together with single-cell transcriptomes in three sequential steps by (i) co-expression analysis, (ii) target gene motif and ChIP-seq track enrichment analysis and (iii) regulon activity evaluation (Figure 2A). Each regulon consists of a TF with its predicted target genes (co-expressed genes with an enriched TF motif), altogether forming a regulon. pySCENIC identified 142 regulons that characterize the GRNs of the human adult pancreas (Figure 2B, C, Supplementary Table S7). Multiple regulons identified here as active in the pancreas correspond to TF binding motifs enriched in accessible chromatin in the pancreas, assessed by both ATAC-seq of FACS-purified pancreatic cells (113) and scATAC-seq of human pancreatic cells (114), supporting the validity of the approach (Supplementary Figure S2A, B).

UMAP visualization based on the activity of 142 regulons in non-diabetic and type 2 diabetic pancreata revealed groups of cells that differ from one another based on their regulatory activity (Figure 2B, C). In particular, there are distinct regulatory states for exocrine and endocrine pancreatic lineages, stellate and endothelial cells (Figure 2B, C). Endocrine cell types clustered together, indicating shared regulatory states, while exocrine cell types formed two distinct clusters. Stellate and endothelial cells differed most from other cell types in their regulatory states. These results are consistent with previous analyses (5,10,82) and are also in line with our findings based on gene expression analysis (Figure 1D). As expected, regulons active in endocrine cell types include RFX6, PAX6 and NEUROD1 (Figure 2D–G). These TFs have reported roles in endocrine cell fate commitment and maintenance of cell identity throughout adult life (48,51,52,115). Using iRegulon for visualization, many of the NEUROD1 target genes identified here have been previously linked to beta cell survival and

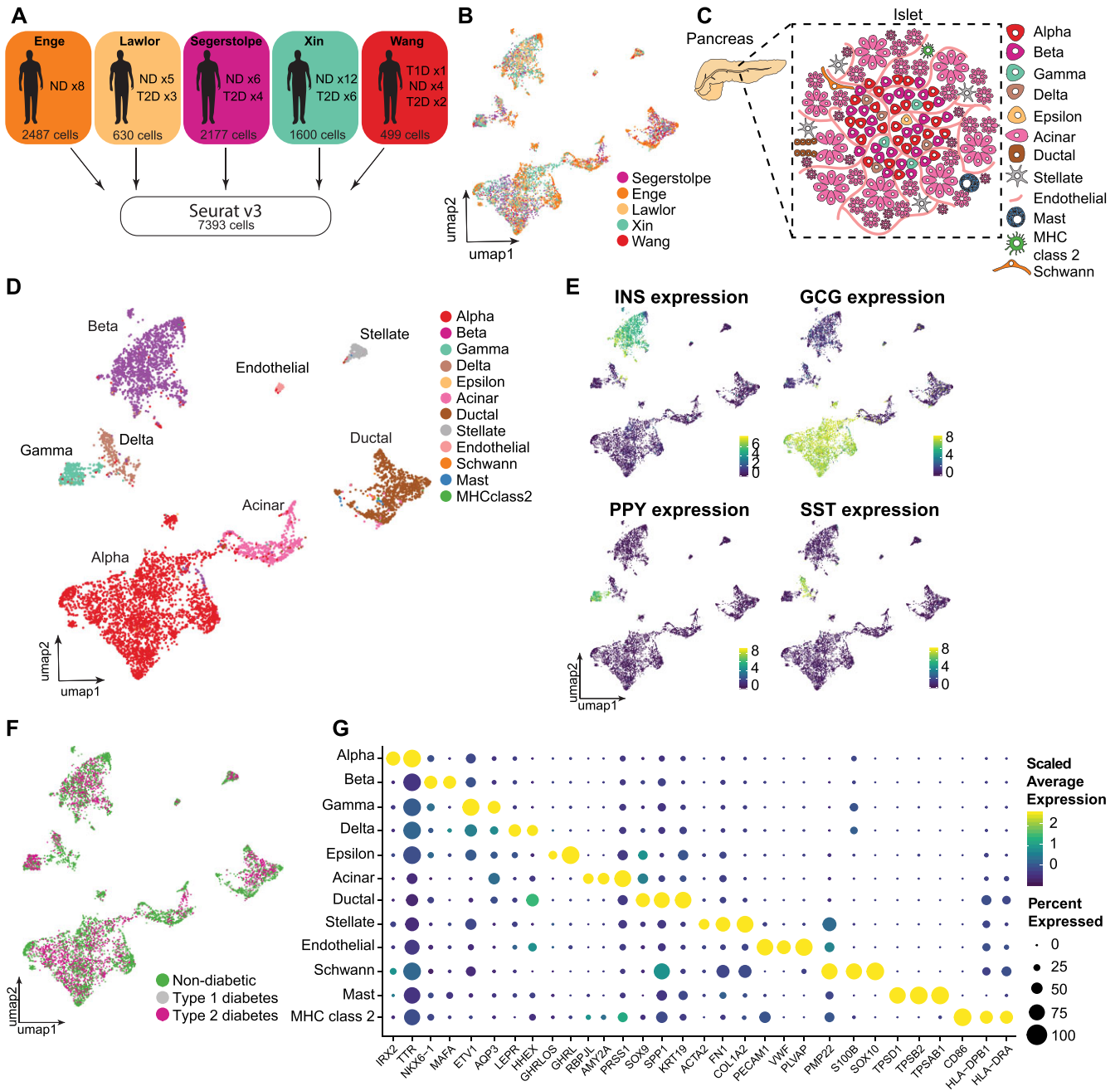


Figure 1. Integrated analysis of scRNA-seq identifies 12 pancreatic cell types. (A) Schematic of workflow used in this paper. Cells from five public datasets were processed uniformly from raw SRA files and integrated, resulting in one dataset of 7393 cells of 51 individuals. (B) Integrated gene expression based UMAP of 7393 single cells annotated by dataset of origin. (C) Schematic overview of diverse cell types in the human adult pancreas. Created with BioRender.com (D) Integrated gene expression based UMAP of 7393 single cells annotated by cell type. (E) Integrated gene expression based UMAP of 7393 single cells colored by non-integrated INS, GCG, PPY and SST expression. (F) Integrated gene expression based UMAP of 7393 single cells annotated by disease status. (G) Bubble plot showing various known marker genes across all annotated cell types. The bubble size is proportional to the percentage of cells that express a specific marker gene with the color scale representing the average non-integrated scaled gene expression within the specific cell population.

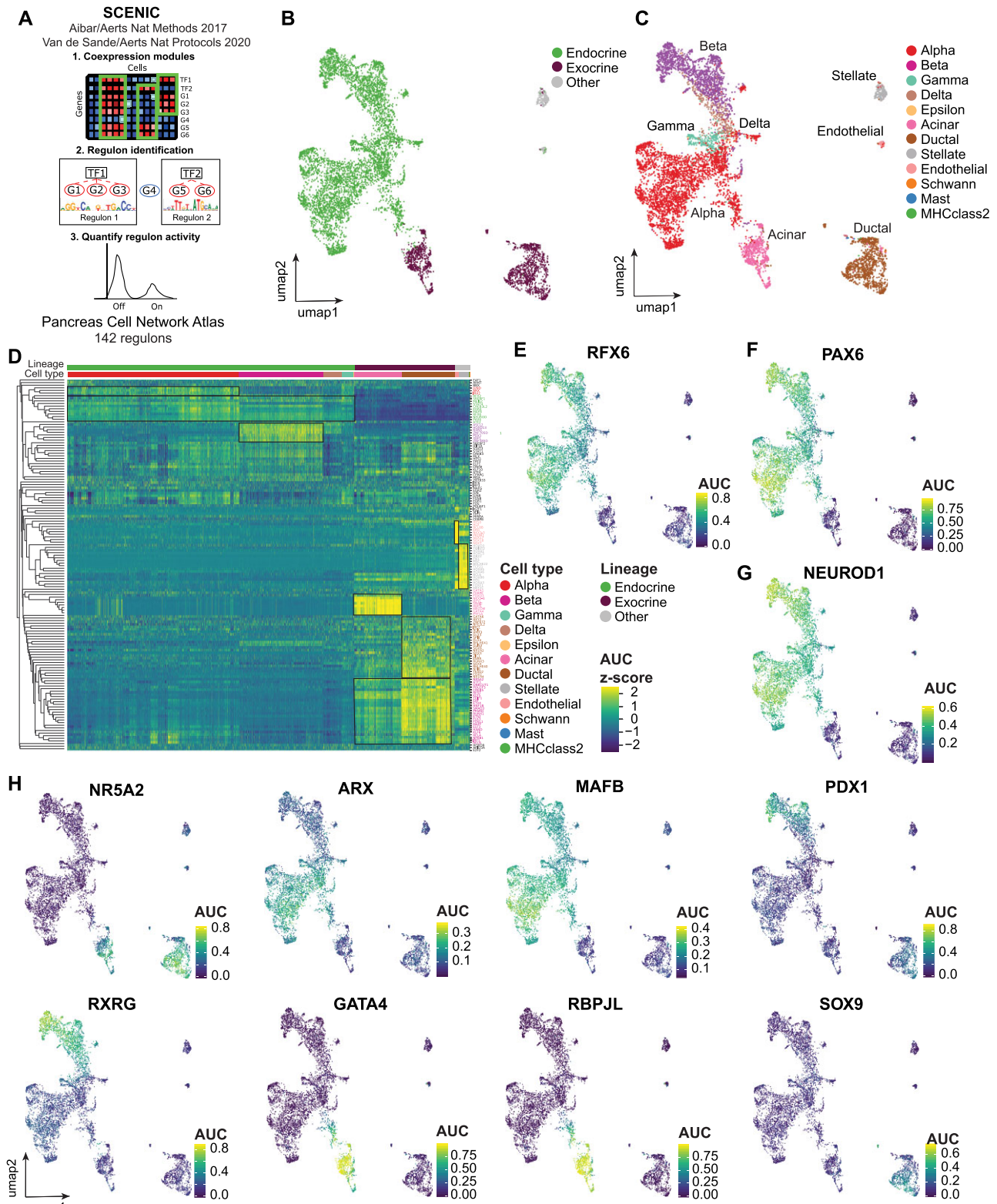


Figure 2. Reconstruction of gene regulatory networks in the human adult pancreas. (A) Schematic overview of the pySCENIC workflow used in this study. (B, C) Regulon activity based UMAP of 7393 single cells colored by pancreatic lineage (B) and cell type annotation (C). Endocrine cells include alpha, beta, epsilon, gamma and delta cells. Exocrine cells include acinar and ductal cells. Other cells represent schwann, MHC class 2, mast, stellate and endothelial cells. (D) Heatmap based on unsupervised clustering of all 142 regulons (rows) for 4795 non-diabetic cells (columns). Color scaling is based on a z-score calculated based on the activity of each regulon. (E–G) Regulon activity based UMAP colored by the regulon activity of RFX6 (E), PAX6 (F), NEUROD1 (G). (H) Regulon activity based UMAP colored by the regulon activity of NR5A2, ARX, MAFB, PDX1, RXRG, GATA4, RBPJL and SOX9.

function, such as SNAP25, TSPAN2, ELAVL4, PLCXD3 and NRNX1 (116–120) (Supplementary Figure S2C). Interestingly, other NEUROD1 target genes are reported to be involved in cell fate specification during endocrine pancreas development such as PAX6, NKX2.2, INSM1 and HDAC6, suggesting an overlap in NEUROD1 target genes in adult life and embryonic development (115,121,122). Clustering all cells based on the activity of all regulons identified regulatory modules (Figure 2D, black squares). In the exocrine pancreas, one regulatory module, containing NR5A2, was shared between acinar and ductal cells, although with a tendency for increased regulon activity in ductal cells (Figure 2D, H). Other exocrine regulons included ONECUT1, REST and HNF1B, with reported roles in exocrine development (123,124) and the adult exocrine pancreas (125,126) (Figure 2D). In summary, this analysis confirms the expected separation of exocrine and endocrine cells with distinct gene regulatory programs, and identifies known and novel candidate regulators of pancreas cell states.

Several regulatory modules are shared between different cell types within the endocrine and exocrine pancreas. Additionally, each cell type is defined by cell type-specific regulatory modules (Figure 1D). In the endocrine pancreas, alpha and beta cells shared endocrine regulons (MAFB, MEIS2), whereas we observed distinct activities for ARX and IRX2 regulons in alpha cells and RXRG and PDX1 in beta cells (Figure 2D, H), expanding previous findings (82). Using iRegulon for visualization, PDX1 target genes include SLC6A17, PDIA6 and ABHD3, which have been reported to control insulin release (127,128) (Supplementary Figure S2D). Interestingly, gamma and delta cells overlapped with alpha and beta cells, respectively, suggesting a shared regulatory state (Figure 2C–D). This includes shared regulon activity for ARX in gamma and alpha and PDX1 in beta and delta cells (Figure 2D, H), consistent with their reported expression in published scRNA-seq studies (5,6,10). GATA4 and RBPJL, known acinar-specific TFs (129,130), were highly active in acinar cells (Figure 2H). Similarly, ductal cells were characterized by highly active SOX9 and POU2F3 regulons, in line with previous literature (55,131) (Figure 2D,H). In sum, this analysis confirms that alpha, beta, acinar and ductal cells are characterized by the activity of distinct combinations of active TFs that form gene regulatory modules.

In conclusion, the network approach recovers many of the expected regulators of pancreatic cellular identity allowing for the comprehensive characterization of the gene regulatory state of all major human adult pancreatic cell types.

Prediction of regulators of endocrine cell identity and cell states in the human adult pancreas

A comprehensive network analysis provides an opportunity to predict and identify regulators of cell identity and cell states. To identify regulons with highly cell type-specific activities within the human adult non-diabetic pancreas, we calculated regulon specificity scores (RSS) (Supplementary Table S1) (81). The RSS utilizes Jensen–Shannon divergence to measure the similarity between the probability distribution of the regulon's enrichment score and cell type

annotation wherein outliers receive a higher RSS and are therefore considered cell type-specific (81). It can therefore be used to rank the activity of TFs within specific cell types.

Among the top regulons identified in alpha cells, we recover well known regulators of alpha and endocrine cell fate such as ARX, IRX2, PAX6, MAFB, NEUROD1 and RFX6 (Figure 3A,B) (48–52,132,133). In addition, we identified JUND, EGR4, SREBF1 and STAT4 that have not yet been implicated in alpha cell identity or state. EGR1 (but not EGR4) has been shown to transcriptionally regulate GCG (134) as well as the PDX1 promoter in beta cells (135). STAT4 and JUND have been described respectively in pancreatic tissue in general and in beta cells but not in alpha cells (136–138) (Figure 3B, C). Interestingly, these TFs were also highly expressed in primary alpha cells found in the PANC-DB scRNA-seq dataset (139) (Supplementary Figure S3A). These TFs respond to the JNK and EGFR signaling pathways and may have important physiological functions. Both JUND and the JUND/JNK signaling pathway have been implicated in pancreatic cancer (140,141). Immunocytochemistry of the human adult pancreas confirmed the presence of nuclear JUND in islets (Figure 3Di). We also detected nuclear JUND protein in a subset of hiPSCs subjected to beta cell differentiation (Figure 3E, F). Surprisingly, we also detected JUND protein in ductal cells, despite lower JUND regulon activity in this cell type (Figure 3C, Dii). Thus, protein expression does not necessarily mean that the TF is active in a given cell type. We also confirmed the expression of putative JUND target genes in primary alpha cells using the PANC-DB scRNA-seq dataset (139) (Supplementary Figure S3B). Nevertheless, these results show that JUND is present and active in a subset of pancreatic cell types in the human adult pancreas and hiPSC-derived islet cells. Altogether, this analysis predicts TFs active in human alpha cells, recovering known as well as new candidate TFs.

Among the top regulons identified in beta cells, we retrieved well-known as well as new candidate regulators of beta and endocrine cell identity. Known TFs include RXRG, PDX1, NEUROD1, PAX6 and RFX6 (42,51,52,115,142,143) (Figure 3G, H). In addition, we found that ZNF705D, ASCL2, BHLHE41 and HOXD13 were highly ranked regulons (Figure 3H, I). HOXD13 and BHLHE41 have been shown to be present in the exocrine pancreas (144,145). We confirmed that these TFs were also expressed in primary beta cells of the PANC-DB scRNA-seq dataset (139) (Supplementary Figure S3C). Interestingly, ASCL2 has been reported to interact with β -catenin of the Wnt pathway; the latter has an established role in endocrine fate specification during *in vitro* differentiation (146–148). Many putative target genes of ASCL2 including PDX1, INS, ABCC8, FOXA1, KCNK16, FXYD2 are directly related to glucose sensing and beta cell identity, in line with the beta cell-specific regulatory activity of ASCL2 (Supplementary Figure S3D) (117,149,150). FXYD2 γ a, a regulatory subunit of the Na⁺-K⁺-ATPase, is a transcript exclusively expressed in human beta cells (151). Immunohistochemistry of human adult pancreas sections showed that ASCL2 is expressed in INS⁺ beta and islet cells (Figure 3J). Surprisingly, ASCL2 was mainly localized to the cytoplasm (Figure 3J), which is unexpected for TFs which tend

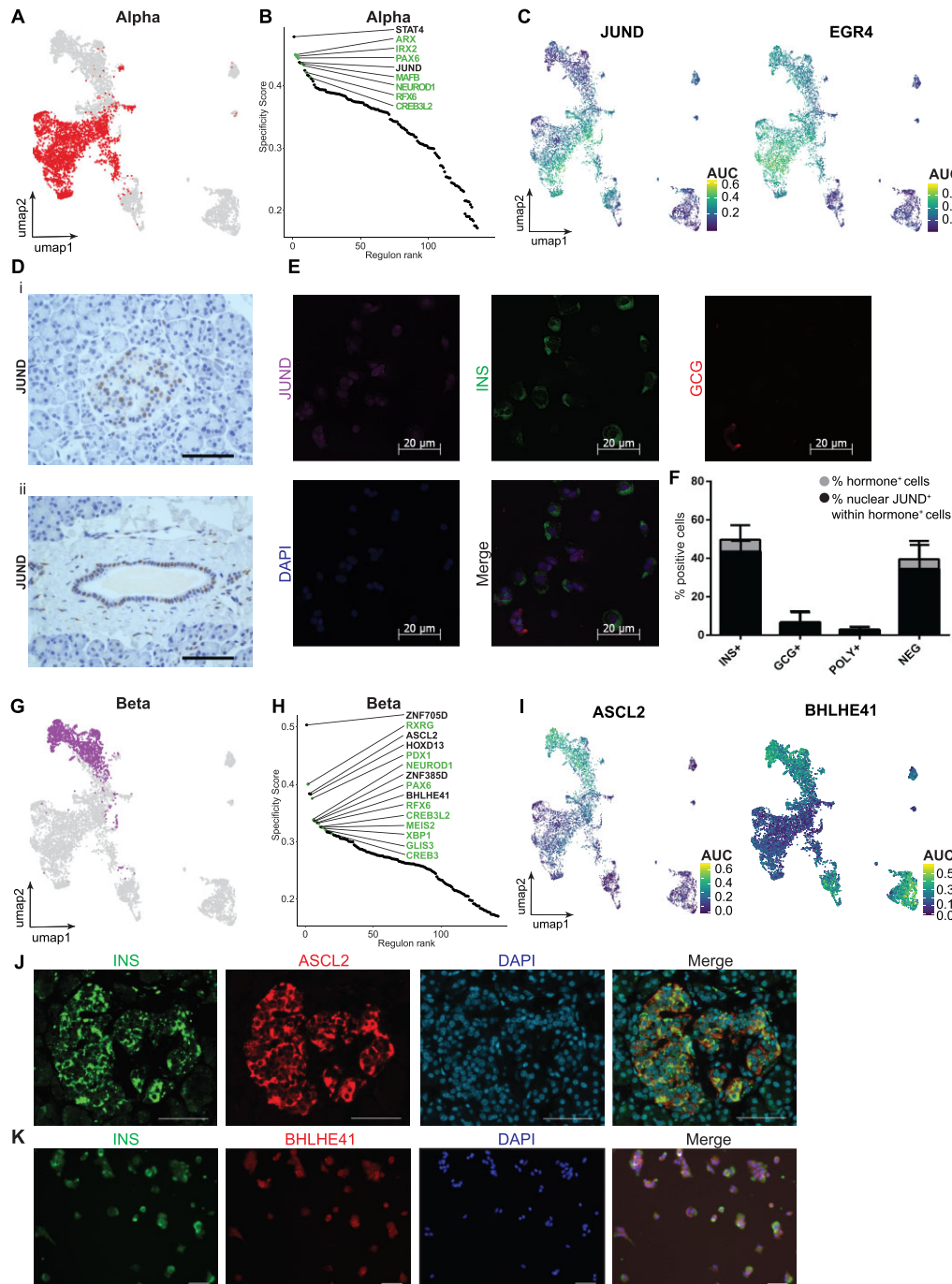


Figure 3. Prediction of regulators of endocrine cell identity in the human adult pancreas. (A) Regulon activity based UMAP of 7393 single cells with the alpha cell population highlighted. (B) Top 10 ranked regulons in non-diabetic alpha cells based on regulon specificity score (RSS). Known cell type specific regulons are colored green. (C) Regulon activity based UMAP colored by the regulon activity of JUND and EGR4 showing the cell type specificity of regulons. (D) Immunohistochemical evaluation of JUND in healthy human adult pancreata showing nuclear JUND expression in alpha, beta (i) and ductal (ii) cells. Representative images are shown ($n = 3$ individuals), Scale bar: $50 \mu\text{m}$. (E) Immunofluorescence evaluation of JUND, INS, GCG and SST at stage 7 of hiPSC-islet differentiation. Box indicates a GCG⁺ cell with nuclear JUND expression. Representative images examined for JUND (green), INS (red), GCG (purple) and DAPI (blue, nuclei counterstaining) are shown ($n = 3$ hiPSC-islet differentiations). Scale bar: $50 \mu\text{m}$. (F) The percentage of cells with nuclear JUND expression within the INS⁺, GCG⁺, polyhormonal and INS⁻/GCG⁻ cell populations. Results are shown as the normalized mean \pm s.d. ($n = 3$ hiPSC-islet differentiations). (G) Regulon activity based UMAP of 7393 single cells with the beta cell population highlighted. (H) Top 10 ranked regulons in non-diabetic beta cells based on regulon specificity score (RSS). Known cell type specific regulons are colored green. (I) Regulon activity based UMAP colored by the regulon activity of ASCL2 and BHLHE41 showing the cell type specificity of regulons. (J) Immunohistochemical evaluation of ASCL2 in healthy human adult pancreata showing cytoplasmic ASCL2 expression in mainly beta cells. Representative images examined for INS (green), ASCL2 (red) and DAPI (blue, nuclei counterstaining) are shown ($n = 3$ individuals), Scale bar: $50 \mu\text{m}$. (K) Immunohistochemical evaluation of BHLHE41 at stage 7 of hiPSC-beta cell differentiation showing nuclear BHLHE41 expression in beta cells. Representative images examined for INS (green), BHLHE41 (red) and DAPI (blue, nuclei counterstaining) are shown ($n = 2$ hiPSC-islet differentiations), Scale bar: $50 \mu\text{m}$.

to localize to the nucleus (152). Cytoplasmic localization of ASCL2 has been reported in the context of colon and breast cancer (153,154). Immunohistochemistry of hiPSC-derived islet cells showed that BHLHE41 is expressed both in nuclei and cytoplasm of INS+ beta cells (Figure 3K). We also confirmed the expression of putative BHLHE41 target genes using the PANC-DB scRNA-seq dataset (139) (Supplementary Figure S3E). These results implicate additional TFs including ASCL2 and BHLHE41 in the regulation of beta cell identity and cell states. They also illustrate the value of network analyses to increase our understanding of the biology of the human pancreas.

In summary, GRN analysis and regulon ranking allowed us to pinpoint both known and previously unknown candidate regulators of pancreatic endocrine cell identity and cell states, providing a resource for further investigation of their roles in cellular identity, state and function.

BHLHE41 and JUND depletion in hiPSC-derived islet cells

To examine the effect of perturbation of candidate TFs in the human adult pancreas, we selected two TFs for targeting with siRNAs in hiPSC-derived islet cells, an *in vitro* pancreatic islet model (35). JUND was identified as a regulator of oxidative stress and lipotoxicity in beta cells (137,138) but its potential role in alpha cells remains unknown. BHLHE41 was of interest due to its role in circadian rhythm regulation (155) but its putative impact on cell identity and cell state in the human pancreas has not yet been investigated.

To gain insight into how candidate TF knockdown affects the transcriptome, cell identity and cell states, we differentiated hiPSCs into islet cells using a protocol that we have previously described (Supplementary Figure S4A–H, Supplementary Table S2–S3, (97)), then performed siRNA knockdown of JUND or BHLHE41, followed by scRNA-seq 72 h post siRNA transfection (Figure 4A). We confirmed that both JUND and BHLHE41 transcript levels were decreased in siRNA-transfected cells (Figure 4B, C, Supplementary Figure S5A, B). BHLHE41 and JUND knockdown did not result in global gene expression changes suggesting that perturbation of these TFs is compatible with the maintenance of GRNs (Figure 4D).

We next sought to annotate cell types within our scRNA-seq dataset using clustering analyses and the expression of well-established cell type specific markers (Figure 4E–F). This led to the identification of nine populations among the hiPSC islet cells: alpha, beta, delta, enterochromaffin, endocrine progenitor, exocrine and non-pancreatic cells (Figure 4E), in line with previous publications (11,22,29–35,79).

To cross-reference our data with primary islets and published islet differentiation experiments, we integrated the dataset with previously described data (35) (Supplementary Figure S5C, D). Most of the cell types identified in our dataset grouped together with previous datasets (35,36) and away from the primary human islet dataset (8) suggesting that our cell populations are transcriptionally similar to previously published datasets.

Next, we investigated whether BHLHE41 or JUND perturbation altered cell type proportions (Figure 4G, Sup-

plementary Table S8). The number of sc-beta and sc-alpha cells remained unchanged upon either BHLHE41 and JUND perturbation, suggesting that TF knockdown did not result in specific loss of these cells (Figure 4G). Sc-enterochromaffin cells are a known off-target population generated during the differentiation of hiPSCs towards the beta cell fate (34,35). Recently, sc-enterochromaffin cells were found to more closely resemble a pre-beta cell population in the fetal pancreas (79). Interestingly, both BHLHE41 and JUND deficiency tended to increase the number of sc-enterochromaffin cells (25% siBH, 23% siJU versus 19% siControl (siCT)) (Figure 4G).

Next, we examined which genes were affected by JUND or BHLHE41 depletion in hiPSC-derived islet cells by determining differentially expressed genes compared to the control condition (adjusted P -value < 0.05, \log_2 fold change = 0.1). In sc-alpha cells, the expression of key beta cell genes INS, PCSK1, HADH and NKX2.2 (66) was increased upon JUND depletion (Figure 4H). Additionally, GO analysis identified ‘insulin secretion’ and ‘alpha cell to beta cell conversion’ as top enriched pathways upon JUND depletion (Supplementary Figure S5E). Upon BHLHE41 depletion, sc-beta cells increased expression of multiple ion channels and proteins involved in endocrine cell electrical activity and granule exocytosis such ABCC8 (156), CACNA1A (157), KCNK16 (150) and VAMP2 (158). In contrast, the expression of key beta cell markers INS, SCG3 and TTR (159) decreased (Figure 4I). GO analysis identified ‘Type 2 diabetes’ as an enriched pathway upon BHLHE41 depletion (Supplementary Figure S5F). pySCENIC can be used to predict putative target genes of TFs (Supplementary Table S9) (112,91). We assessed if JUND and BHLHE41 knockdown altered the expression of their predicted target genes (Supplementary Table S9). The expression of the majority of BHLHE41 (10/12) and JUND (24/32) target genes in sc-alpha and sc-beta cells seemed to be unaffected upon siRNA treatment suggesting that the effect of TF knockdown was specific to a few genes (Supplementary Figure S5G, H).

BHLHE41 deficiency induces apoptosis in human adult pancreatic islets

GRNs were computed using primary pancreas scRNA-seq data (6–10), but the validation experiments were carried out in hiPSC-derived islet cells. Since differences exist between hiPSC-derived islets and primary islets (35,97), we next assessed whether JUND and BHLHE41 modulate cell states in primary islets, using a knockdown approach. 72h after siRNA transfection into primary islet cells, we confirmed that JUND and BHLHE41 transcript levels were decreased (Figure 5A–C, Supplementary Figure S6A, B). While JUND depletion did not affect human islet cell viability (Pearson correlation, $R = -0.34$, $p = 0.23$), reduced BHLHE41 transcript levels did correlate with increased apoptosis (Spearman correlation, $R = -0.6$, $P = 0.025$) (Figure 5D, E, Supplementary Figure S5C). Interestingly, these results suggest that BHLHE41 promotes the survival of primary islets.

JUND depletion had no significant effect on transcript levels of alpha cell marker genes GCG, MAFB and ARX,

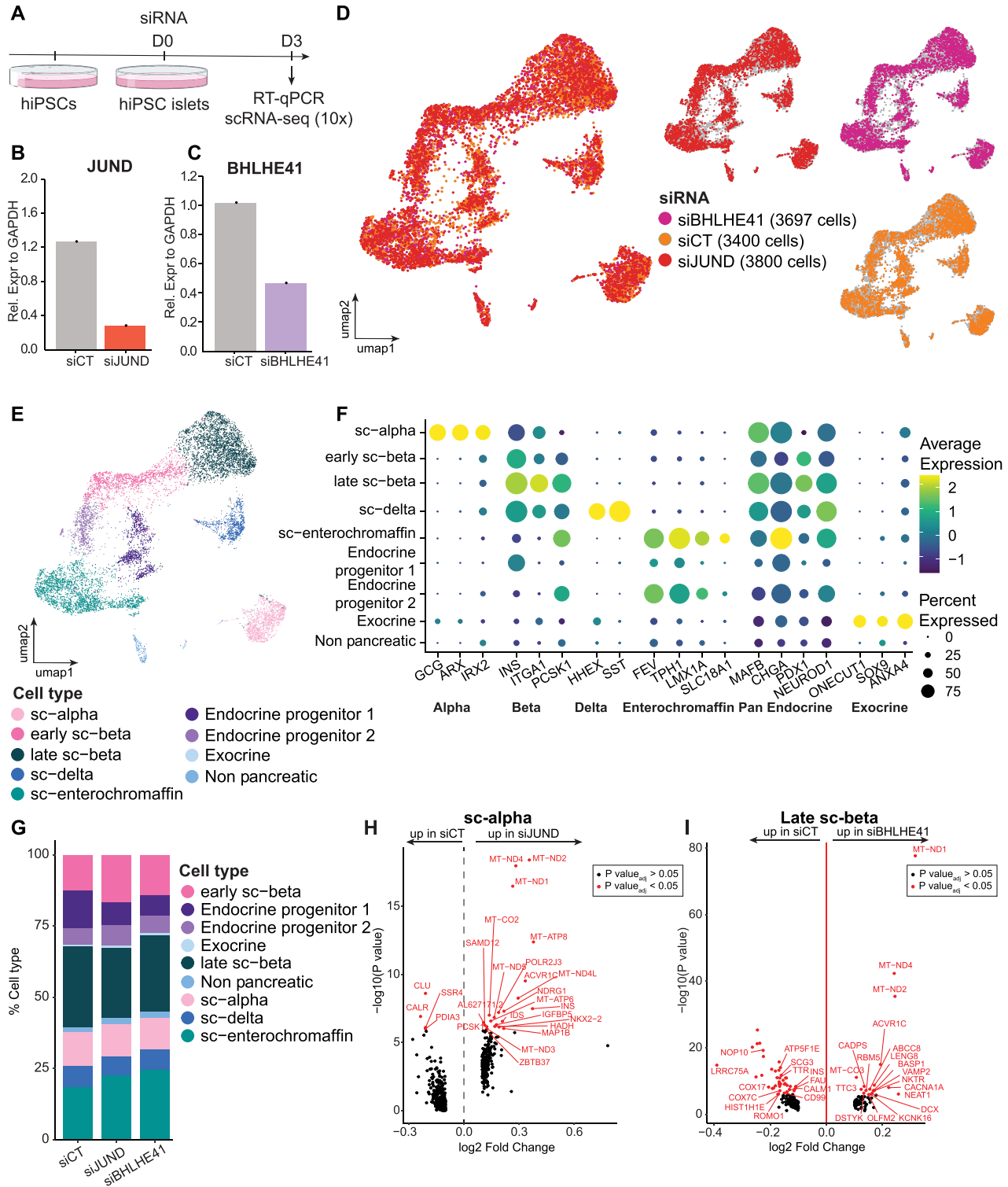


Figure 4. BHLHE41 and JUND depletion in hiPSC-derived islet cells. (A) Scheme of siRNA mediated BHLHE41 and JUND knockdown in hiPSC-islet cells. Created with BioRender.com (B, C) JUND (B) and BHLHE41 (C) transcript level 72h after siRNA transfection by RT-qPCR. Results are relative to the expression of GAPDH (arbitrary units) ($n = 1$ hiPSC-islet differentiation). (D, E) Gene expression based UMAP of 10897 single cells annotated by siRNA transfection (D) and cell type (E). (F) Bubble plot showing the expression of various known marker genes across all annotated cell types. The bubble size is proportional to the percentage of cells that express a specific marker gene with the color scale representing the average scaled gene expression within the specific cell population. (G) Percentage of different cell types in each siRNA condition. (H) Volcano plot of differentially expressed genes in siCT and siJUND treated sc-alpha cells. Genes with an adjusted P -value < 0.05 are shown in red. Black represents genes that were not found to differ significantly between siRNA transfected groups. (I) Volcano plot of differentially expressed genes in siCT and siBHLHE41 transfected late sc-beta cells. Genes with an adjusted P -value < 0.05 are shown in red. Black represents genes that were not found to differ significantly between siRNA treated groups.

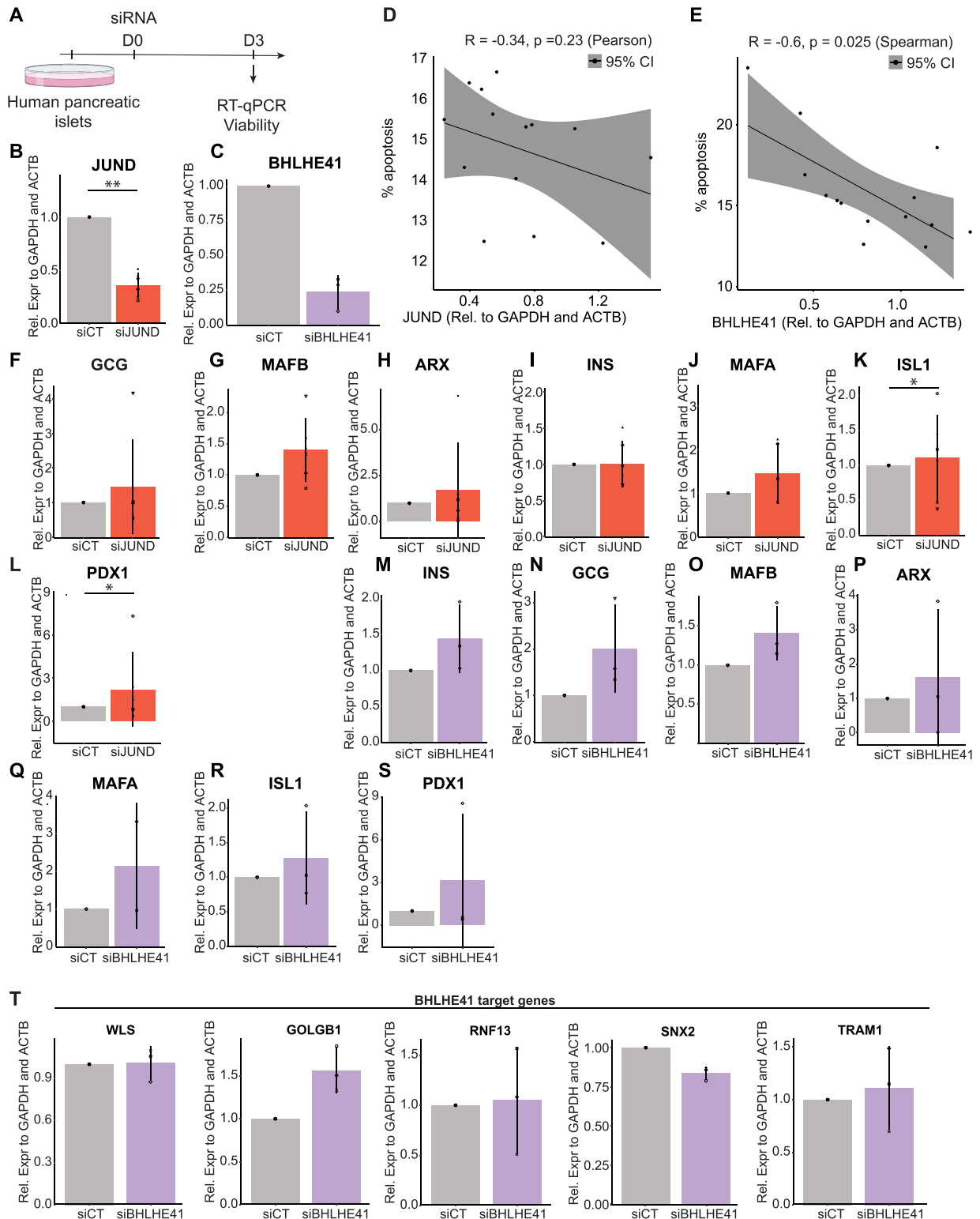


Figure 5. BHLHE41 deficiency induces apoptosis in human adult pancreatic islets. (A) Scheme of siRNA mediated BHLHE41 and JUND knockdown in primary pancreatic islets. Created with BioRender.com (B, C) JUND (B) and BHLHE41 (C) transcript levels 72 h after siRNA transfection. (D) Pearson correlation between the percentage of apoptotic cells and JUND transcript level. (E) Spearman correlation between the percentage of apoptotic cells and BHLHE41 transcript level. (F–L) GCG (F), MAFB (G), ARX (H), INS (I), MAFA (J), ISL1 (K) and PDX1 (L) transcript levels 72 h after JUND siRNA transfection. $n = 6$ islet preparations (M–S) INS (M), GCG (N), MAFB (O), ARX (P), MAFA (Q), ISL1 (R) and PDX1 (S) transcript levels 72 h after BHLHE41 siRNA transfection. $n = 3$ islet preparations (T) Transcript level of BHLHE41 putative target genes WLS, GOLGB1, RNF13, SNX2 and TRAM1 72 hours post transfection in primary human islets. $n = 3$ islet preparations. * $P < 0.05$, ** $P < 0.01$ (Wilcoxon rank sum test with FDR correction compared to siCT). Results are shown as the normalized mean \pm s.d. Each symbol represents one independent experiment.

nor on beta cell marker genes *INS* and *MAFA*, while *ISL1* and *PDX1* transcript levels increased (Figure 5F–L). Interestingly, *BHLHE41* siRNA treatment tended to increase *INS*, *GCG* and *MAFB* transcript levels, albeit not significantly (Figure 5M–O). We did not observe changes in *ARX*, *MAFA*, *ISL1* and *PDX1* transcript levels (Figure 5P–S). We further assessed whether the expression of predicted *BHLHE41* targets changed upon *BHLHE41* knockdown. There was a trend for increased *GOLGB1* expression, a component of the Golgi complex that is pivotal for proper insulin secretion (Figure 5T) (160). Altogether, these data suggest that *BHLHE41* deficiency induced apoptosis, increased *INS*, *GCG* and *MAFB* levels and altered transcript levels of a predicted target gene in primary islets.

Prediction of regulators of exocrine cell identity and cell states in the human adult pancreas

The comprehensive network analysis above also provides an opportunity to predict and identify regulators of exocrine cell identity and cell states.

We identified known and new TFs in acinar cells. Among the top acinar-specific regulons, we recovered well known regulators of acinar and exocrine cell identity such as *PTF1A*, *RBPJL*, *GATA4* and *NR5A2* (53,123,130,161) (Figure 6A, B). These findings are in line with a recent study that used single-nucleus RNA-seq on pancreatic acinar tissue (162) and the expression of TFs in acinar cells of the PANC-DB scRNA-seq dataset (139) (Supplementary Figure S7A). Furthermore, we identified *MECOM*, *HEYL* and *TGIF1* as highly ranked regulons (Figure 6B/C). Interestingly, *MECOM* expression has been linked to acinar cell dedifferentiation which increases susceptibility to malignancy (163). The loss of *TGIF1* has been linked to pancreatic ductal adenocarcinoma progression making further exploration of these regulons interesting in the context of cancer biology (164,165). Ectopic expression of *Tgif2* (but not *Tgif1*) reprograms mouse liver cells towards a pancreas progenitor state (166). *HEYL* is a reported Notch signaling target gene in *NGN3*⁺ exocrine cells (167). We confirmed nuclear expression of *HEYL* in human acinar and islet cells (Figure 6Di/ii, donor information can be found in Supplementary Table S5) by immunohistochemistry, in agreement with elevated *HEYL* regulon activity in acinar cells (Figure 6C).

Top ranked regulons in ductal cells included well known regulators of ductal and exocrine cell identity such as *POU2F3*, *NR5A2* and *HNF1B* (123,125,131) (Figure 6E, F). In addition, we observed *CDX2* and *PPARD* as highly specific ductal regulons (Figure 6F, G). Both *PPARD* and *CDX2* have been reported to be involved in human pancreatic ductal carcinoma, warranting further functional studies (168,169). We confirmed the expression of predicted TFs within ductal cells of the PANC-DB scRNA-seq dataset (139) (Supplementary Figure S7B).

In summary, GRN analysis and regulon ranking allowed us to pinpoint both known and predicted candidate regulators of pancreatic exocrine GRNs and cell identity. Specifically, we identified *HEYL* as a candidate TF that might be implicated in regulating acinar cell identity, warranting further investigation.

Type 2 diabetes does not affect the global gene regulatory state of alpha and beta cells

Finally, we compared single cell regulon profiles from type 2 diabetic and non-diabetic individuals to identify potential shifts in regulatory state and increase insight into the impact of type 2 diabetes at the GRN level. Unsupervised clustering revealed that type 2 diabetes does not appear to cause global shifts in the gene regulatory landscape in alpha and beta cells, in agreement with a previous study (82) (Figure 7A, B). For UMAP regions where cells appeared to cluster together based on disease state, we found that the donor was an underlying factor, emphasizing the importance of studying large patient numbers (Supplementary Figure S8A, B).

Comparing the average regulon activity of type 2 diabetic and non-diabetic alpha cells did identify differentially activated regulons (Figure 7C, Supplementary Table S10). Type 2 diabetic alpha cells exhibit a significantly higher *EGR1* regulon activity (Figure 7D, E). *EGR1* was shown to be essential for basal and gastrin-dependent glucagon gene transactivation in alpha cells, consistent with observed chronic hyperglucagonemia in type 2 diabetes (170) (Figure 7D). *HIF1A*, which has a significantly higher average regulon activity in type 2 diabetic alpha cells, has been linked to hypoxia-induced beta cell dysfunction in type 2 diabetes warranting the study of *HIF1A* in non-beta cells (171) (Figure 7E).

Comparing the average regulon activity of type 2 diabetic and non-diabetic beta cells did not identify differentially activated regulons, suggesting that the global gene regulatory state is not greatly affected (Figure 7F, Supplementary Table S11). Higher regulon activity of *RXRG* in type 2 diabetic beta cells could explain the beneficial effect of *RXR* agonists on enhancing glucose-stimulated insulin secretion in type 2 diabetes (142) (Figure 7G). There was no decrease in *PAX6*, *MAFB*, *NKX6.1* or *PDX1* regulon activity, contrary to what has been reported in type 2 diabetes mouse models (172) and human type 2 diabetic beta cells (173).

Altogether, these findings imply that the activity of a subset of TFs may be affected in alpha cells in type 2 diabetes, possibly affecting the activity of a subset of regulons in alpha cells without altering the general beta cell gene regulatory state.

An interactive online resource for visualization of the human adult pancreas cell network atlas

To enable users to easily navigate the human pancreatic cell network atlas, we provide a loom file that allows for the visualization and exploration of the data using the web-based portal SCoPe (76) (.loom file and tutorial available at http://scope.aertslab.org/#/PancreasAtlas*/welcome and <https://github.com/pasquelab/scPancreasAtlas>). Features such as cell type annotation as defined in this paper, gene expression and regulon activity, can be explored on the regulon and gene expression based UMAPs. This resource enables users to select and visualize up to three genes or regulons simultaneously and select subsets of cells for downstream analyses. Target genes of a specific regulon can be downloaded to facilitate further exploration, for example in iRegulon or gene ontology analysis (73). A list of predicted target genes of all 142 regulons can also be found in Supplementary Table S9.

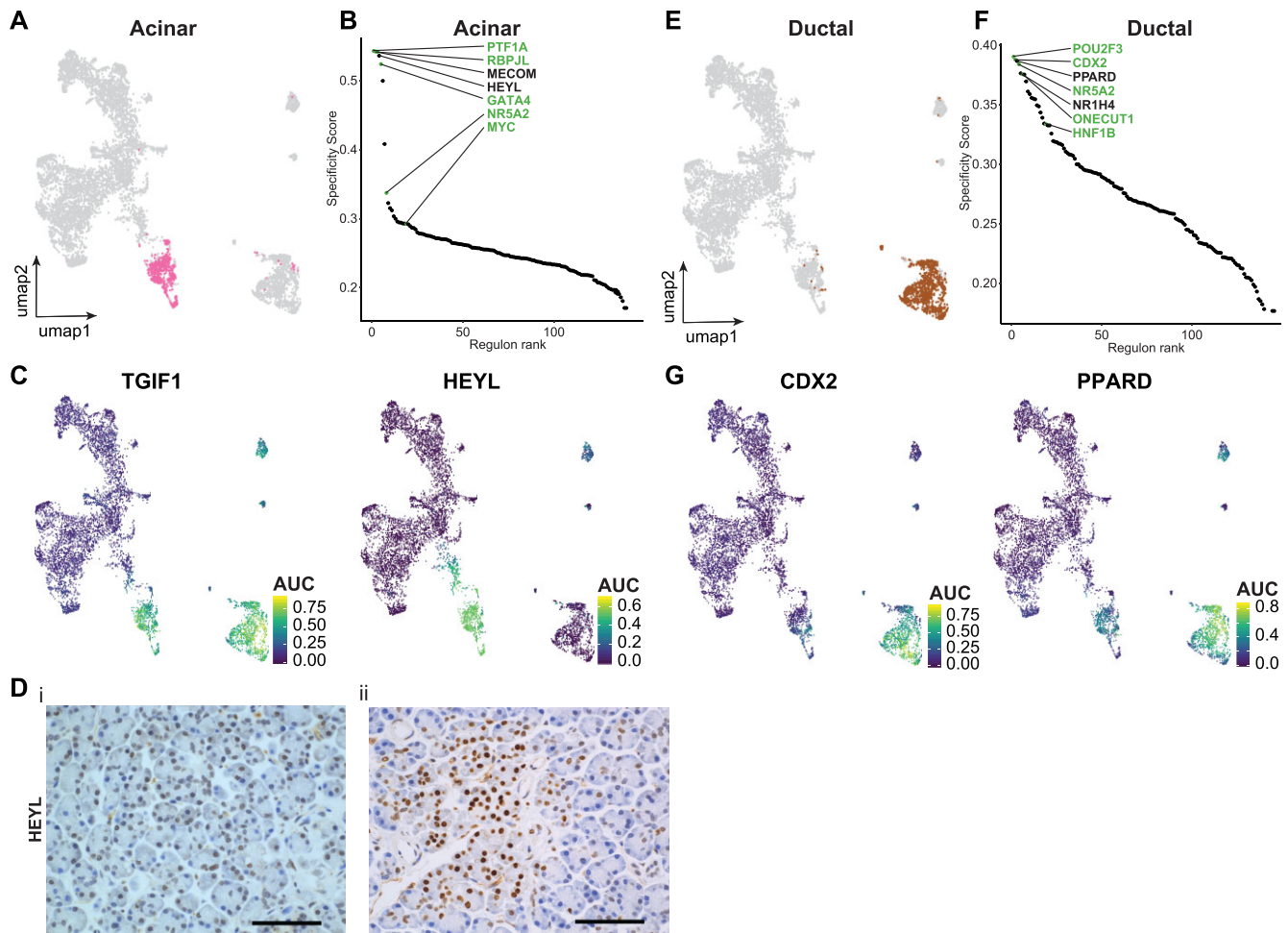


Figure 6. Prediction of regulators of exocrine cell identity in the human adult pancreas. (A) Regulon activity based UMAP of 7393 single cells with the acinar cell population highlighted. (B) Top 10 ranked regulons in non-diabetic acinar cells based on regulon specificity score (RSS). Known cell type specific regulons are colored green. (C) Regulon activity based UMAP colored by the regulon activity of TGIF1 and HEYL showing the cell type specificity of regulons. (D) Immunohistochemical evaluation of HEYL in healthy human adult pancreata showing nuclear HEYL expression in acinar (i) and islet (ii) cells. Representative images are shown ($n = 3$ individuals), Scale bar: 50 μm . (E) Regulon activity based UMAP of 7393 single cells with the ductal cell population highlighted. (F) Top 10 ranked regulons in non-diabetic ductal cells based on regulon specificity score (RSS). Known cell type specific regulons are colored green. (G) Regulon activity based UMAP colored by the regulon activity of CDX2 and PPAR showing the cell type specificity of regulons.

Furthermore, a list of target genes can be manually defined to compute the activity of a custom regulon. This resource can be used to further study cell identity, cell states, GRNs and gene regulation in the context of the pancreas.

DISCUSSION

In this resource, we take advantage of integration strategies and new computational tools to reconstruct an integrated cell and GRN atlas of the human adult pancreas from single-cell transcriptome data. This approach provides a comprehensive analysis of the gene regulatory logic underlying cellular identity and cell states in the human adult pancreas in a broad range of individuals, limiting the influence of inter-donor variability. We recovered known regulators of pancreatic cell identity and uncovered predicted candidate regulators of cell identity and cell states that can be further investigated for their roles in cellular identity, state and function. By validating regulon analyses and creating

an easily accessible interactive online resource which allows for the exploration of the gene regulatory state of 7393 cells from 51 individuals, this approach extends beyond previous gene regulatory studies in the human adult pancreas (82).

The present analysis identified regulators of pancreatic development, function and survival that are known to be critical in humans because loss-of-gene function causes pancreatic agenesis or young onset diabetes. For example, PTF1A and GATA4, whose loss of function are linked to pancreatic agenesis and neonatal diabetes (58,60,174), were among the top acinar-specific regulons (Figure 6). In addition, monogenic diabetes related genes PDX1 (175), NEUROD1 (64), PAX6 (63), RFX6 (51,176) and GLIS3 (62) were among the top beta cell-specific regulons (Figure 3 and Supplementary Table S1).

Several top regulons in endocrine but not exocrine cells are TFs involved in endoplasmic reticulum stress signaling (Supplementary Table S1). CREB3 and CREB3L2 are non-canonical endoplasmic reticulum stress transducers that are

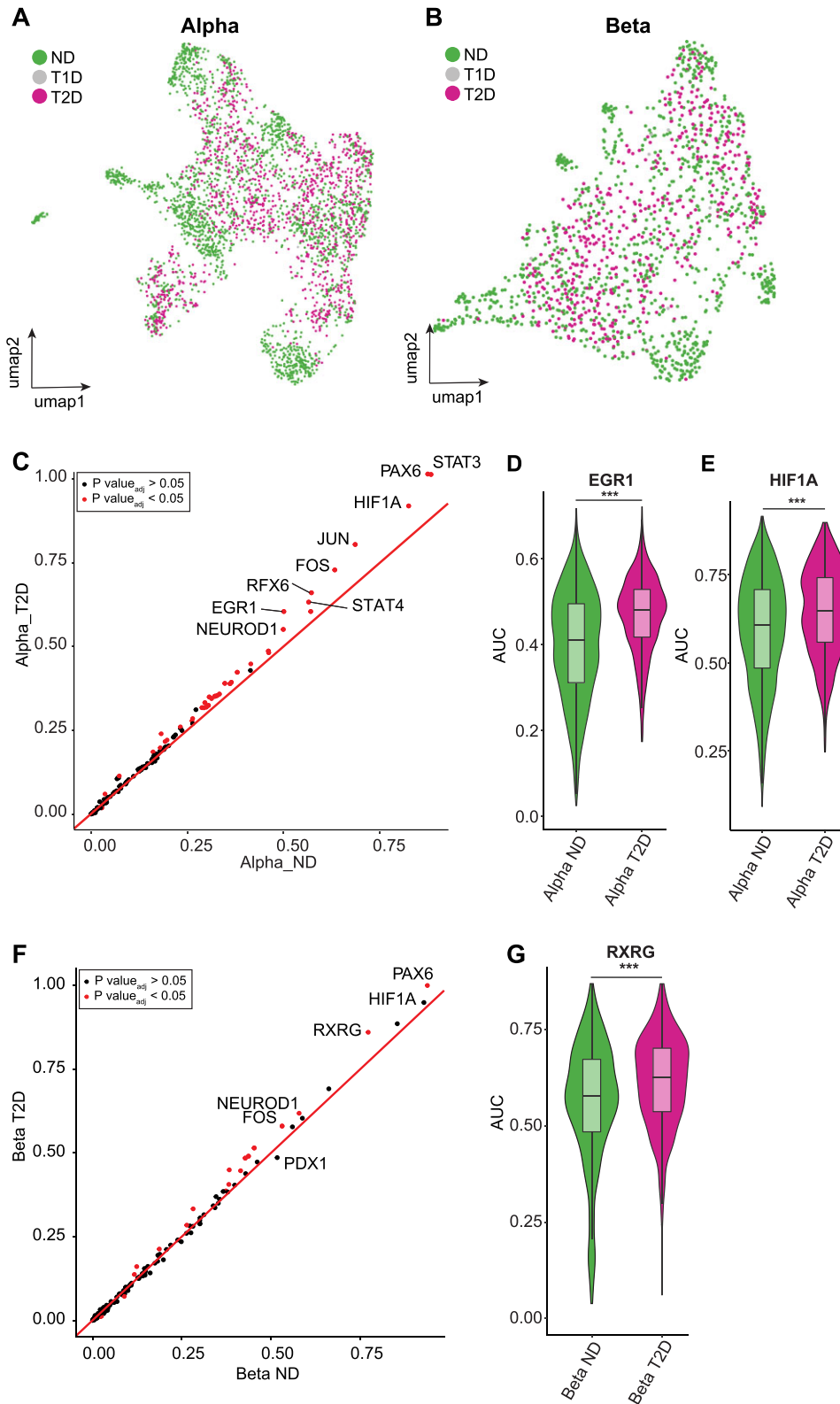


Figure 7. Disease state does not majorly impact regulon activity in alpha and beta cells. (A) Regulon based UMAP of 3215 alpha cells annotated by disease status. (B) Median regulon activity in non-diabetic (ND) alpha cells versus type 2 diabetic (T2D) alpha cells. Regulons with an adjusted P -value < 0.05 are shown in red. Black represents regulons that were not found to differ significantly between ND and T2D cells. (C, D) Violinplot of EGR1 (C) and HIF1A (D) regulon activity. (E) Regulon based UMAP of 1538 beta cells annotated by disease status. (F) Median regulon activity in ND beta cells versus T2D beta cells. Regulons with an adjusted p -value < 0.05 are shown in red. Black represents regulons that were not found to differ significantly between ND and T2D cells. (G) Violinplot of RXRG regulon activity. *** $P < 0.0001$ non-parametric Wilcoxon rank sum test. In C,D and G, boxes correspond to the 25th and 75th quartiles, horizontal lines to the median, and whiskers extend to 1.5 times the interquartile range.

induced in human islets and clonal beta cells upon exposure to the saturated fatty acid palmitate (177). Interestingly, SREBF1 and -2 undergo similar endoplasmic reticulum exit and proteolytic processing in the Golgi as these endoplasmic reticulum stress transducers, but they do so in response to changes in endoplasmic reticulum cholesterol content; both also have high regulon activity in alpha and beta cells. XBP1 is abundantly expressed in the exocrine and endocrine pancreas (178), but the XBP1 regulon has its highest specificity in beta cells. ATF3 and ATF4 are TFs that are activated upon eIF2 α phosphorylation, an endoplasmic reticulum stress response pathway to which no less than 5 monogenic forms of diabetes belong (179). Our data underscore the importance of these TFs for endocrine pancreatic cell identity.

Disruptions of circadian clock genes within the pancreas have been linked to impaired glucose tolerance and type 2 diabetes (180–182). The mammalian circadian clock consists of transcriptional oscillators that coordinate behavior and metabolism within a 24h light-dark cycle. The core loop consists of BMAL1-CLOCK that activate clock-controlled genes, including PER and CRY genes, which in turn form complexes that inhibit CLOCK-BMAL1 mediated transcription upon entry in the nucleus (183). Here, we investigated the role of BHLHE41, a transcriptional repressor of CLOCK-BMAL1 that in turn activates clock target genes (184,185). We found that BHLHE41 deficiency induced apoptosis in human islets. This finding is consistent with reports of apoptosis caused by disrupting the circadian rhythm of diabetic rats (186). The high level of redundancy between different clock genes could help explain the limited transcriptional effects of the depletion of a single clock gene (187). It is speculated that this genetic and functional redundancy of clock genes ensures tight control and entrainment of circadian rhythm (188–190).

Given that we predict regulators of cell identity and cell states in the human pancreas, it will be interesting to expand this analysis to embryonic development of the pancreas (3,20–22,191). Our work may also be beneficial in guiding the *in vitro* differentiation of pancreatic cell types and minimize the emergence of off-target cell populations such as sc-enterochromaffin cells. For example, the emergence of SST-positive cells together with beta-like cells at the end of *in vitro* differentiation could be explained by the overlap in regulatory states between beta and delta cells (5). A better understanding of the regulatory logic underlying the control of beta cell fate through these GRN analyses may help improve or facilitate future applications in regenerative medicine (29,192–195). Alternatively, many TFs such as ASCL2, MECOM, PPAR δ , GATA6 and CDX2 are linked to pancreatic cancer making the exploration of GRNs interesting in the context of cancer biology (153,154,164,168,169,196,197). Recent reports have stratified type 2 diabetes patients based on age at diagnosis, BMI, HbA1c and insulin secretion and sensitivity, and identified subtypes with different genetic predisposition, treatment response, disease progression and complication rates (198). Hence, it would be interesting to assess differences in gene regulatory state and gene expression profiles of alpha and beta cells between different type 2 diabetic subgroups.

Taken together, our GRN atlas, containing 51 individuals, provides a valuable resource for future studies on human pancreas homeostasis, donor variability, development, and disease including type 2 diabetes and pancreatic cancer. Finally, our results provide new insights into the activity of TFs and gene regulation in the human adult pancreas from a gene regulatory perspective.

Limitations of the study

It is important to note that pySCENIC is a stochastic algorithm that does not produce precisely the same regulons for repeated runs, limiting reproducibility when comparing different datasets and when SCENIC is used multiple times on the same dataset (112,92). To mitigate this uncertainty, we ran the full pySCENIC pipeline five times and only kept consistent regulons with the highest regulon activity. Alternatively, SCENIC could be automated to be run hundreds of times to further mitigate stochasticity (112). The performance of pySCENIC and other GRN inference methods suffers due to the large amount of dropout events in scRNA-seq data warranting caution when interpreting results (199). This could explain the absence of well-established pancreas TFs such as MAFA (200), MNX1 (66), NEUROG3 (201), FOXA2 (54) and NKX2-2 (202) in this analysis. Nevertheless, in support of the validity of our findings, ATAC-seq, the literature and immunohistochemistry of human pancreas sections corroborate several pySCENIC predictions reported here such as BHLHE41, JUND and HEYL (137,138,167). Chen and colleagues underline the importance of using large sample sizes to derive the most accurate network inference possible (199), highlighting the importance of dataset integration to increase the number of cells analyzed. However, we cannot exclude that integration of datasets may mask differences between datasets of origins. In the future, it will be interesting to extend these analyses to include many more cells and patients, and to develop methods for better differential regulon analysis across datasets. Despite current caveats, GRN analysis has enabled the capture of biological relevant information (203).

In this work, we tested the effect of BHLHE41 and JUND knockdown in both hiPSC-derived and primary islets. The absence of complete BHLHE41 and JUND depletion could explain the limited effect on candidate target genes. CRISPR knockout approaches could be used in the future to mitigate this limitation (204). Additionally, we cannot exclude that the dispersion of cells and 2D culture prior to siRNA transfection affects islet cell behavior (205).

One additional limitation of this study is the assumption that all TFs bind their binding motifs in the promoters of expressed genes. However, TF binding can be restricted to a subset of TF motifs in the genome due to influence of chromatin processes including the presence of nucleosomes as well as DNA methylation. Therefore, additional approaches such as single cell multi-omics that capture additional layers of genome regulation will be helpful to increase our understanding of gene regulation in the context of the human pancreas. Recently developed computational tools including SCENIC + and CellOracle could help towards this goal (74,75).

DATA AVAILABILITY

Further information and requests for resources should be directed to and will be fulfilled by the Lead Contact, Vincent Pasque (vincent.pasque@kuleuven.be). This study did not generate new unique reagents. Regulon data, raw and integrated gene expression matrices and the .loom file are available in the Gene Expression Omnibus (GEO) repository under accession code GSE156490 [<https://www.ncbi.nlm.nih.gov/geo/query/acc.cgi?acc=GSE156490>] and GSE218547 [<https://www.ncbi.nlm.nih.gov/geo/query/acc.cgi?acc=GSE218547>]. A SCoPe tutorial is available at <https://github.com/pasquelab/scPancreasAtlas>. This study did not generate any new software; questions about data analysis should be directed to the Lead Contact, Vincent Pasque (vincent.pasque@kuleuven.be).

SUPPLEMENTARY DATA

Supplementary Data are available at NARGAB Online.

ACKNOWLEDGEMENTS

We thank Stein Aerts, Kristofer Davie and the Stein Aerts lab for discussions and creating the permanent SCoPe link, Shengbao Suo for sharing the MATLAB script for calculating the regulon specificity score, the Flemish Supercomputer Center (VSC) and Leuven Stem Cell Institute. We thank Stein Aerts for feedback on the manuscript.

Author contributions: Conceived project, V.P., L.V. Performed experiments, F.F., A.A.S., M.V.H., T.O. Analyses, F.F., L.V., A.A.S., T.O., M.V.H., T.H., A.R., T.H., T.S., T.R. scRNA-seq analyses, L.V., X.Y., A.J., J.C. ATAC-seq analysis, L.V. Resources, M.C., J.K.C. Wrote manuscript, L.V., V.P. and M.C. with input from all authors. Supervision, V.P.

FUNDING

Research in the Pasque laboratory was supported by the Research Foundation– Flanders [FWO ; Odysseus Return Grant G0F7716N to V.P.; FWO grants G0C9320N and G0B4420N to V.P.]; KU Leuven Research Fund [BOFZAP starting grant StG/15/021BF to V.P. and C1 grant C14/21/119 to V.P.]; FWO SB Ph.D. Fellowship to L.V. [1S29419N]; Pandarome project 40007487 [G0I7822N] (funded by the FWO and F.R.S.-FNRS) under the Excellence of Science (EOS) programme (to M.C., V.P.); Research in the Cnop lab was also funded by the Fonds National de la Recherche Scientifique (FNRS) (to M.C., F.F.); Marie Skłodowska-Curie Actions Fellowship from the European Union's Horizon 2020 research and innovation programme under the Marie Skłodowska-Curie [801505 to T.S.]; Walloon Region SPW-EERWin2Wal project BetaSource and the Francophone Foundation for Diabetes Research (sponsored by the French Diabetes Federation, Abbott, Eli Lilly, Merck Sharp & Dohme and Novo Nordisk) (to M.C.); European Foundation for the Study of Diabetes/Boehringer Ingelheim European Research Programme on 'Multi-System Challenges in Diabetes' (to M.C. and F.F.); Innovative Medicines Initiative 2 Joint Undertaking [115797] (INNODIA); this Joint Undertaking receives support from

the Union's Horizon 2020 research and innovation program and 'EFPIA' (European Federation of Pharmaceutical Industries Associations); 'JDRF' (Juvenile Diabetes Research Foundation); 'The Leona M. and Harry B. Helmsley Charitable Trust'; this manuscript used data acquired from the Human Pancreas Analysis Program (HPAP-RRID:SCR_016202) Database (<https://hpap.pmacs.upenn.edu>); Human Islet Research Network (RRID:SCR_014393) consortium [UC4-DK-112217, U01-DK-123594, UC4-DK-112232, U01-DK-123716]; T.O. was supported by the KU Leuven Research Fund C1 [C14/20/097 to T.R.].
Conflict of interest statement. None declared.

REFERENCES

- Kahn, S.E., Cooper, M.E. and Del Prato, S. (2014) Pathophysiology and treatment of type 2 diabetes: perspectives on the past, present, and future. *Lancet*, **383**, 1068–1083.
- Kamisawa, T., Wood, L.D., Itoi, T. and Takaori, K. (2016) Pancreatic cancer. *Lancet*, **388**, 73–85.
- Han, X., Zhou, Z., Fei, L., Sun, H., Wang, R., Chen, Y., Chen, H., Wang, J., Tang, H., Ge, W. *et al.* (2020) Construction of a human cell landscape at single-cell level. *Nature*, **581**, 303–309.
- Grün, D., Muraro, M.J., Boisset, J.-C., Wiebrands, K., Lyubimova, A., Dharmadhikari, G., van den Born, M., van Es, J., Jansen, E., Clevers, H. *et al.* (2016) De novo prediction of stem cell identity using single-cell transcriptome data. *Cell Stem Cell*, **19**, 266–277.
- Baron, M., Veres, A., Wolock, S.L., Faust, A.L., Gaujoux, R., Vetere, A., Ryu, J.H., Wagner, B.K., Shen-Orr, S.S., Klein, A.M. *et al.* (2016) A single-cell transcriptomic map of the Human and mouse pancreas reveals inter- and intra-cell population structure. *Cell Syst.*, **3**, 346–360.
- Segerstolpe, Å., Palasantza, A., Eliasson, P., Andersson, E.-M., Andréasson, A.-C., Sun, X., Picelli, S., Sabirsh, A., Clausen, M., Bjursell, M.K. *et al.* (2016) Single-cell transcriptome profiling of Human pancreatic islets in health and type 2 diabetes. *Cell Metab.*, **24**, 593–607.
- Wang, Y.J., Schug, J., Won, K.-J., Liu, C., Naji, A., Avrahami, D., Golson, M.L. and Kaestner, K.H. (2016) Single-cell transcriptomics of the Human endocrine pancreas. *Diabetes*, **65**, 3028–3038.
- Xin, Y., Kim, J., Okamoto, H., Ni, M., Wei, Y., Adler, C., Murphy, A.J., Yancopoulos, G.D., Lin, C. and Gromada, J. (2016) RNA sequencing of single Human islet cells reveals type 2 diabetes genes. *Cell Metab.*, **24**, 608–615.
- Enge, M., Efsun Arda, H., Mignardi, M., Beausang, J., Bottino, R., Kim, S.K. and Quake, S.R. (2017) Single-cell analysis of Human pancreas reveals transcriptional signatures of aging and somatic mutation patterns. *Cell*, **171**, 321–330.
- Lawlor, N., George, J., Bolisetty, M., Kursawe, R., Sun, L., Sivakamasundari, V., Kycia, I., Robson, P. and Stitzel, M.L. (2017) Single-cell transcriptomes identify human islet cell signatures and reveal cell-type-specific expression changes in type 2 diabetes. *Genome Res.*, **27**, 208–222.
- Augsornworawat, P., Maxwell, K.G., Velazco-Cruz, L. and Millman, J.R. (2020) Single-cell transcriptome profiling reveals β cell maturation in stem cell-derived islets after transplantation. *Cell Rep.*, **32**, 108067.
- Augsornworawat, P. and Millman, J.R. (2020) Single-cell RNA sequencing for engineering and studying human islets. *Curr. Opin. Biomed. Eng.*, **16**, 27–33.
- He, S., Wang, L.-H., Liu, Y., Li, Y.-Q., Chen, H.-T., Xu, J.-H., Peng, W., Lin, G.-W., Wei, P.-P., Li, B. *et al.* (2020) Single-cell transcriptome profiling of an adult human cell atlas of 15 major organs. *Genome Biol.*, **21**, 294.
- Fasolino, M., Schwartz, G.W., Patil, A.R., Mongia, A., Golson, M.L., Wang, Y.J., Morgan, A., Liu, C., Schug, J., Liu, J. *et al.* (2022) Single-cell multi-omics analysis of human pancreatic islets reveals novel cellular states in type 1 diabetes. *Nat. Metab.*, **4**, 284–299.
- Stanescu, D.E., Yu, R., Won, K.-J. and Stoffers, D.A. (2017) Single cell transcriptomic profiling of mouse pancreatic progenitors. *Physiol. Genomics*, **49**, 105–114.

16. Byrnes, L.E., Wong, D.M., Subramaniam, M., Meyer, N.P., Gilchrist, C.L., Knox, S.M., Tward, A.D., Ye, C.J. and Sneddon, J.B. (2018) Lineage dynamics of murine pancreatic development at single-cell resolution. *Nat. Commun.*, **9**, 3922.
17. Scavuzzo, M.A., Hill, M.C., Chmielowiec, J., Yang, D., Teaw, J., Sheng, K., Kong, Y., Bettini, M., Zong, C., Martin, J.F. *et al.* (2018) Endocrine lineage biases arise in temporally distinct endocrine progenitors during pancreatic morphogenesis. *Nat. Commun.*, **9**, 3356.
18. Duvall, E., Benitez, C.M., Tellez, K., Enge, M., Pauerstein, P.T., Li, L., Baek, S., Quake, S.R., Smith, J.P., Sheffield, N.C. *et al.* (2022) Single-cell transcriptome and accessible chromatin dynamics during endocrine pancreas development. *Proc. Natl. Acad. Sci. U.S.A.*, **119**, e2201267119.
19. Muraro, M.J., Dharmadhikari, G., Grün, D., Groen, N., Dielen, T., Jansen, E., van Gurp, L., Engelse, M.A., Carlotti, F., de Koning, E.J.P. *et al.* (2016) A single-cell transcriptome atlas of the Human pancreas. *Cell Syst.*, **3**, 385–394.
20. Cao, J., O'Day, D.R., Pliner, H.A., Kingsley, P.D., Deng, M., Daza, R.M., Zager, M.A., Aldinger, K.A., Blecher-Gonen, R., Zhang, F. *et al.* (2020) A human cell atlas of fetal gene expression. *Science*, **370**, eaba7721.
21. la O Sean, D., Liu, Z., Sun, H., Yu, S.K., Wong, D.M., Chu, E., Rao, S.A., Eng, N., Peixoto, G., Bouza, J. *et al.* (2022) Single-cell multi-omic roadmap of Human fetal pancreatic development. bioRxiv doi: <https://doi.org/10.1101/2022.02.17.480942>, 18 February 2022, preprint: not peer reviewed.
22. Gonçalves, C.A., Larsen, M., Jung, S., Stratmann, J., Nakamura, A., Leuschner, M., Hersemann, L., Keshara, R., Perlman, S., Lundvall, L. *et al.* (2021) A 3D system to model human pancreas development and its reference single-cell transcriptome atlas identify signaling pathways required for progenitor expansion. *Nat. Commun.*, **12**, 3144.
23. Xu, Y., Zhang, T., Zhou, Q., Hu, M., Qi, Y., Xue, Y., Wang, L., Nie, Y., Bao, Z. and Shi, W. (2022) A single-cell transcriptome atlas of human early embryogenesis. bioRxiv doi: <https://doi.org/10.1101/2021.11.30.470583>, 01 December 2021, preprint: not peer reviewed.
24. Lin, L., Zhang, Y., Qian, W., Liu, Y., Zhang, Y., Lin, F., Liu, C., Lu, G., Song, Y., Song, J. *et al.* (2021) Single-cell transcriptome lineage tracing of human pancreatic development identifies distinct developmental trajectories of alpha and beta cells. bioRxiv doi: <https://doi.org/10.1101/2021.01.14.426320>, 15 January 2021, preprint: not peer reviewed.
25. (2023) Single-cell transcriptomic and spatial landscapes of the developing human pancreas. *Cell Metab.*, **35**, 184–199.
26. Liu, H., Yang, H., Zhu, D., Sui, X., Li, J., Liang, Z., Xu, L., Chen, Z., Yao, A., Zhang, L. *et al.* (2014) Systematically labeling developmental stage-specific genes for the study of pancreatic β -cell differentiation from human embryonic stem cells. *Cell Res.*, **24**, 1181–1200.
27. Kang, R.B., Li, Y., Rosselot, C., Zhang, T., Siddiq, M., Rajbhandari, P., Stewart, A.F., Scott, D.K., Garcia-Ocana, A. and Lu, G. (2023) Single-nucleus RNA sequencing of human pancreatic islets identifies novel gene sets and distinguishes beta-cell subpopulations with dynamic transcriptome profiles. *Genome Med.*, **15**, 30.
28. Wigger, L., Barovic, M., Brunner, A.-D., Marzetta, F., Schöniger, E., Mehl, F., Kipke, N., Friedland, D., Burdet, F., Kessler, C. *et al.* (2021) Multi-omics profiling of living human pancreatic islet donors reveals heterogeneous beta cell trajectories towards type 2 diabetes. *Nat Metab.*, **3**, 1017–1031.
29. Rezaia, A., Bruin, J.E., Arora, P., Rubin, A., Batushansky, I., Asadi, A., O'Dwyer, S., Quiskamp, N., Mojibian, M., Albrecht, T. *et al.* (2014) Reversal of diabetes with insulin-producing cells derived in vitro from human pluripotent stem cells. *Nat. Biotechnol.*, **32**, 1121–1133.
30. Hrvatin, S., O'Donnell, C.W., Deng, F., Millman, J.R., Pagliuca, F.W., DiIorio, P., Rezaia, A., Gifford, D.K. and Melton, D.A. (2014) Differentiated human stem cells resemble fetal, not adult, β cells. *Proc. Natl. Acad. Sci. U.S.A.*, **111**, 3038–3043.
31. Zhu, Z., Li, Q.V., Lee, K., Rosen, B.P., González, F., Soh, C.-L. and Huangfu, D. (2016) Genome editing of lineage determinants in Human pluripotent stem cells reveals mechanisms of pancreatic development and diabetes. *Cell Stem Cell*, **18**, 755–768.
32. Högbe, N.J., Maxwell, K.G., Augsornworawat, P. and Millman, J.R. (2021) Generation of insulin-producing pancreatic β cells from multiple human stem cell lines. *Nat. Protoc.*, **16**, 4109–4143.
33. Peterson, Q.P., Veres, A., Chen, L., Slama, M.Q., Kenty, J.H.R., Hassoun, S., Brown, M.R., Dou, H., Duffy, C.D., Zhou, Q. *et al.* (2020) A method for the generation of human stem cell-derived alpha cells. *Nat. Commun.*, **11**, 2241.
34. Veres, A., Faust, A.L., Bushnell, H.L., Engquist, E.N., Kenty, J.H.-R., Harb, G., Poh, Y.-C., Sintov, E., Gürtler, M., Pagliuca, F.W. *et al.* (2019) Charting cellular identity during human in vitro β -cell differentiation. *Nature*, **569**, 368–373.
35. Balboa, D., Barsby, T., Lithovius, V., Saarimäki-Vire, J., Omar-Hmeadi, M., Dyachok, O., Montaser, H., Lund, P.-E., Yang, M., Ibrahim, H. *et al.* (2022) Functional, metabolic and transcriptional maturation of human pancreatic islets derived from stem cells. *Nat. Biotechnol.*, **40**, 1042–1055.
36. Krentz, N.A.J., Lee, M.Y.Y., Xu, E.E., Sproul, S.L.J., Maslova, A., Sasaki, S. and Lynn, F.C. (2018) Single-cell transcriptome profiling of mouse and hESC-derived pancreatic progenitors. *Stem Cell Rep.*, **11**, 1551–1564.
37. Budnik, B., Straubhaar, J., Neveu, J. and Shvartsman, D. (2022) In-depth analysis of proteomic and genomic fluctuations during the time course of human embryonic stem cells directed differentiation into beta cells. *Proteomics*, **22**, e2100265.
38. Augsornworawat, P., Högbe, N.J., Ishahak, M., Schmidt, M.D., Marquez, E., Maestas, M.M., Veronese-Paniagua, D.A., Gale, S.E., Miller, J.R., Velazco-Cruz, L. *et al.* (2023) Single-nucleus multi-omics of human stem cell-derived islets identifies deficiencies in lineage specification. *Nat. Cell Biol.*, **25**, 904–916.
39. Fiers, M.W.E.J., Fiers, M.W.E., Minnoye, L., Aibar, S., González-Blas, C.B., Atak, Z.K. and Aerts, S. (2018) Mapping gene regulatory networks from single-cell omics data. *Brief Funct Genomics*, **17**, 246–254.
40. Ohno, S. (1979) The number of genes in the mammalian genome and the need for master regulatory genes. In: Ohno, S. (ed.) *Major Sex-Determining Genes*. Springer Berlin Heidelberg, Berlin, Heidelberg, pp. 17–21.
41. Dassay, R., Naidoo, S. and Cerf, M.E. (2016) Transcription factor regulation of pancreatic organogenesis, differentiation and maturation. *Islets*, **8**, 13–34.
42. Zhou, Q., Brown, J., Kanarek, A., Rajagopal, J. and Melton, D.A. (2008) In vivo reprogramming of adult pancreatic exocrine cells to beta-cells. *Nature*, **455**, 627–632.
43. Shih, H.P., Seymour, P.A., Patel, N.A., Xie, R., Wang, A., Liu, P.P., Yeo, G.W., Magnuson, M.A. and Sander, M. (2015) A gene regulatory network cooperatively controlled by Pdx1 and Sox9 governs lineage allocation of foregut progenitor cells. *Cell Rep.*, **13**, 326–336.
44. Nishimura, W., Takahashi, S. and Yasuda, K. (2015) MafA is critical for maintenance of the mature beta cell phenotype in mice. *Diabetologia*, **58**, 566–574.
45. Gradwohl, G., Dierich, A., LeMeur, M. and Guillemot, F. (2000) Neurogenin3 is required for the development of the four endocrine cell lineages of the pancreas. *Proc. Natl. Acad. Sci. U.S.A.*, **97**, 1607–1611.
46. Sussel, L., Kalamaras, J., Hartigan-O'Connor, D.J., Meneses, J.J., Pedersen, R.A., Rubenstein, J.L. and German, M.S. (1998) Mice lacking the homeodomain transcription factor Nkx2.2 have diabetes due to arrested differentiation of pancreatic beta cells. *Development*, **125**, 2213–2221.
47. Sosa-Pineda, B., Chowdhury, K., Torres, M., Oliver, G. and Gruss, P. (1997) The Pax4 gene is essential for differentiation of insulin-producing β cells in the mammalian pancreas. *Nature*, **386**, 399–402.
48. Mastracci, T.L., Anderson, K.R., Papizan, J.B. and Sussel, L. (2013) Regulation of Neurod1 contributes to the lineage potential of Neurogenin3+ endocrine precursor cells in the pancreas. *PLoS Genet.*, **9**, e1003278.
49. Collombat, P., Mansouri, A., Hecksher-Sorensen, J., Serup, P., Krull, J., Gradwohl, G. and Gruss, P. (2003) Opposing actions of Arx and Pax4 in endocrine pancreas development. *Genes Dev.*, **17**, 2591–2603.
50. Artner, I., Le Lay, J., Hang, Y., Elghazi, L., Schisler, J.C., Henderson, E., Sosa-Pineda, B. and Stein, R. (2006) MafB: an

- activator of the glucagon gene expressed in developing islet alpha- and beta-cells. *Diabetes*, **55**, 297–304.
51. Smith, S.B., Qu, H.-Q., Taleb, N., Kishimoto, N.Y., Scheel, D.W., Lu, Y., Patch, A.-M., Grabs, R., Wang, J., Lynn, F.C. *et al.* (2010) Rfx6 directs islet formation and insulin production in mice and humans. *Nature*, **463**, 775–780.
 52. Piccand, J., Strasser, P., Hodson, D.J., Meunier, A., Ye, T., Keime, C., Birling, M.-C., Rutter, G.A. and Gradwohl, G. (2014) Rfx6 maintains the functional identity of adult pancreatic β cells. *Cell Rep.*, **9**, 2219–2232.
 53. Ketola, I., Otonkoski, T., Pulkkinen, M.-A., Niemi, H., Palgi, J., Jacobsen, C.M., Wilson, D.B. and Heikinheimo, M. (2004) Transcription factor GATA-6 is expressed in the endocrine and GATA-4 in the exocrine pancreas. *Mol. Cell. Endocrinol.*, **226**, 51–57.
 54. Lee, K., Cho, H., Rickert, R.W., Li, Q.V., Pulecio, J., Leslie, C.S. and Huangfu, D. (2019) FOXA2 Is required for enhancer priming during pancreatic differentiation. *Cell Rep.*, **28**, 382–393.
 55. Shroff, S., Rashid, A., Wang, H., Katz, M.H., Abbruzzese, J.L., Fleming, J.B. and Wang, H. (2014) SOX9: a useful marker for pancreatic ductal lineage of pancreatic neoplasms. *Hum. Pathol.*, **45**, 456–463.
 56. Sund, N.J., Vatamaniuk, M.Z., Casey, M., Ang, S.-L., Magnuson, M.A., Stoffers, D.A., Matschinsky, F.M. and Kaestner, K.H. (2001) Tissue-specific deletion of Foxa2 in pancreatic β cells results in hyperinsulinemic hypoglycemia. *Genes Dev.*, **15**, 1706–1715.
 57. Gao, T., McKenna, B., Li, C., Reichert, M., Nguyen, J., Singh, T., Yang, C., Pannikar, A., Doliba, N., Zhang, T. *et al.* (2014) Pdx1 maintains β cell identity and function by repressing an α cell program. *Cell Metab.*, **19**, 259–271.
 58. Sellick, G.S., Barker, K.T., Stolte-Dijkstra, I., Fleischmann, C., Coleman, R.J., Garrett, C., Gloyn, A.L., Edghill, E.L., Hattersley, A.T., Wellauer, P.K. *et al.* (2004) Mutations in PTF1A cause pancreatic and cerebellar agenesis. *Nat. Genet.*, **36**, 1301–1305.
 59. Allen, H.L., Flanagan, S.E., Shaw-Smith, C., De Franco, E., Akerman, I., Caswell, R. and International Pancreatic Agenesis Consortium International Pancreatic Agenesis Consortium, Ferrer, J., Hattersley, A.T. and Ellard, S. (2011) GATA6 haploinsufficiency causes pancreatic agenesis in humans. *Nat. Genet.*, **44**, 20–22.
 60. Shaw-Smith, C., De Franco, E., Lango Allen, H., Batlle, M., Flanagan, S.E., Borowiec, M., Taplin, C.E., van Alfen-van der Velden, J., Cruz-Rojo, J., Perez de Nanclares, G. *et al.* (2014) GATA4 mutations are a cause of neonatal and childhood-onset diabetes. *Diabetes*, **63**, 2888–2894.
 61. De Franco, E., Watson, R.A., Weninger, W.J., Wong, C.C., Flanagan, S.E., Caswell, R., Green, A., Tudor, C., Lelliott, C.J., Geyer, S.H. *et al.* (2019) A specific CNOT1 mutation results in a novel syndrome of pancreatic agenesis and holoprosencephaly through impaired pancreatic and neurological development. *Am. J. Hum. Genet.*, **104**, 985–989.
 62. Senée, V., Chelala, C., Duchatelet, S., Feng, D., Blanc, H., Cossec, J.-C., Charon, C., Nicolino, M., Boileau, P., Cavener, D.R. *et al.* (2006) Mutations in GLIS3 are responsible for a rare syndrome with neonatal diabetes mellitus and congenital hypothyroidism. *Nat. Genet.*, **38**, 682–687.
 63. Solomon, B.D., Pineda-Alvarez, D.E., Balog, J.Z., Hadley, D., Gropman, A.L., Nandagopal, R., Han, J.C., Hahn, J.S., Blain, D., Brooks, B. *et al.* (2009) Compound heterozygosity for mutations in PAX6 in a patient with complex brain anomaly, neonatal diabetes mellitus, and microphthalmia. *Am. J. Med. Genet. A*, **149**, 2543–2546.
 64. Rubio-Cabezas, O., Minton, J.A.L., Kantor, I., Williams, D., Ellard, S. and Hattersley, A.T. (2010) Homozygous mutations in NEUROD1 are responsible for a novel syndrome of permanent neonatal diabetes and neurological abnormalities. *Diabetes*, **59**, 2326–2331.
 65. Bonnefond, A., Vaillant, E., Philippe, J., Skrobek, B., Lobbens, S., Yengo, L., Huyvaert, M., Cavé, H., Busiah, K., Scharfmann, R. *et al.* (2013) Transcription factor gene MNX1 is a novel cause of permanent neonatal diabetes in a consanguineous family. *Diabetes Metab.*, **39**, 276–280.
 66. Flanagan, S.E., De Franco, E., Lango Allen, H., Zerah, M., Abdul-Rasoul, M.M., Edge, J.A., Stewart, H., Alamiri, E., Hussain, K., Wallis, S. *et al.* (2014) Analysis of transcription factors key for mouse pancreatic development establishes NKX2-2 and MNX1 mutations as causes of neonatal diabetes in man. *Cell Metab.*, **19**, 146–154.
 67. Takahashi, K. and Yamanaka, S. (2006) Induction of pluripotent stem cells from mouse embryonic and adult fibroblast cultures by defined factors. *Cell*, **126**, 663–676.
 68. Vierbuchen, T., Ostermeier, A., Pang, Z.P., Kokubu, Y., Südhof, T.C. and Wernig, M. (2010) Direct conversion of fibroblasts to functional neurons by defined factors. *Nature*, **463**, 1035–1041.
 69. Lima, M.J., Muir, K.R., Docherty, H.M., McGowan, N.W.A., Forbes, S., Heremans, Y., Heimberg, H., Casey, J. and Docherty, K. (2016) Generation of functional beta-like cells from Human exocrine pancreas. *PLoS One*, **11**, e0156204.
 70. Ghazanfar, S., Bisogni, A.J., Ormerod, J.T., Lin, D.M. and Yang, J.Y.H. (2016) Integrated single cell data analysis reveals cell specific networks and novel coactivation markers. *BMC Syst. Biol.*, **10**, 127.
 71. Matsumoto, H., Kiryu, H., Furusawa, C., Ko, M.S.H., Ko, S.B.H., Gouda, N., Hayashi, T. and Nikaido, I. (2017) SCODE: an efficient regulatory network inference algorithm from single-cell RNA-seq during differentiation. *Bioinformatics*, **33**, 2314–2321.
 72. Lim, C.Y., Wang, H., Woodhouse, S., Piterman, N., Wernisch, L., Fisher, J. and Göttgens, B. (2016) BTR: training asynchronous boolean models using single-cell expression data. *BMC Bioinf.*, **17**, 355.
 73. Janky, R.'s., Verfaillie, A., Imrichová, H., Van de Sande, B., Standaert, L., Christiaens, V., Hulselmans, G., Hertzen, K., Naval Sanchez, M., Potier, D. *et al.* (2014) iRegulon: from a gene list to a gene regulatory network using large motif and track collections. *PLoS Comput. Biol.*, **10**, e1003731.
 74. Kamimoto, K., Stringa, B., Hoffmann, C.M., Jindal, K., Solnica-Krezel, L. and Morris, S.A. (2023) Dissecting cell identity via network inference and in silico gene perturbation. *Nature*, **614**, 742–751.
 75. González-Blas, C.B., De Winter, S., Hulselmans, G., Hecker, N., Matetovici, I., Christiaens, V., Poovathingal, S., Wouters, J., Aibar, S. and Aerts, S. (2022) SCENIC+: single-cell multiomic inference of enhancers and gene regulatory networks. bioRxiv doi: <https://doi.org/10.1101/2022.08.19.504505>, 19 August 2022, preprint: not peer reviewed.
 76. Davie, K., Janssens, J., Koldere, D., De Waegeneer, M., Pech, U., Kreft, L., Aibar, S., Makhzami, S., Christiaens, V., Bravo González-Blas, C. *et al.* (2018) A single-cell transcriptome atlas of the aging drosophila brain. *Cell*, **174**, 982–998.
 77. Wouters, J., Kalender-Atak, Z., Minnoye, L., Spanier, K.I., De Waegeneer, M., Bravo González-Blas, C., Mauduit, D., Davie, K., Hulselmans, G., Najem, A. *et al.* (2020) Robust gene expression programs underlie recurrent cell states and phenotype switching in melanoma. *Nat. Cell Biol.*, **22**, 986–998.
 78. Peng, G., Suo, S., Cui, G., Yu, F., Wang, R., Chen, J., Chen, S., Liu, Z., Chen, G., Qian, Y. *et al.* (2020) Author correction: molecular architecture of lineage allocation and tissue organization in early mouse embryo. *Nature*, **586**, E7.
 79. Zhu, H., Wang, G., Nguyen-Ngoc, K.-V., Kim, D., Miller, M., Goss, G., Kovsky, J., Harrington, A.R., Saunders, D.C., Hopkirk, A.L. *et al.* (2023) Understanding cell fate acquisition in stem-cell-derived pancreatic islets using single-cell multiome-inferred regulomes. *Dev. Cell*, **58**, 727–743.
 80. Talon, I., Janiszewski, A., Theeuwes, B., Lefevre, T., Song, J., Bervoets, G., Vanheer, L., De Geest, N., Poovathingal, S., Allsop, R. *et al.* (2021) Enhanced chromatin accessibility contributes to X chromosome dosage compensation in mammals. *Genome Biol.*, **22**, 302.
 81. Suo, S., Zhu, Q., Saadatpour, A., Fei, L., Guo, G. and Yuan, G.-C. (2018) Revealing the critical regulators of cell identity in the mouse cell atlas. *Cell Rep.*, **25**, 1436–1445.
 82. Kumar, S. and Vinod, P.K. (2019) Single-cell transcriptomic analysis of pancreatic islets in health and type 2 diabetes. *Int. J. Adv. Eng. Sci. Appl. Math.*, **11**, 105–118.
 83. Faerch, K., Hulman, A. and Solomon, T.P.J. (2015) Heterogeneity of pre-diabetes and type 2 diabetes: implications for prediction, prevention and treatment responsiveness. *Curr. Diabetes Rev.*, **12**, 30–41.

84. Dybala, M.P. and Hara, M. (2019) Heterogeneity of the Human pancreatic islet. *Diabetes*, **68**, 1230–1239.
85. Zaharia, O.P., Strassburger, K., Strom, A., Böhnhof, G.J., Karusheva, Y., Antoniou, S., Bódis, K., Markgraf, D.F., Burkart, V., Müssig, K. *et al.* (2019) Risk of diabetes-associated diseases in subgroups of patients with recent-onset diabetes: a 5-year follow-up study. *Lancet Diabetes Endocrinol.*, **7**, 684–694.
86. Dennis, J.M., Shields, B.M., Henley, W.E., Jones, A.G. and Hattersley, A.T. (2019) Disease progression and treatment response in data-driven subgroups of type 2 diabetes compared with models based on simple clinical features: an analysis using clinical trial data. *Lancet Diabetes Endocrinol.*, **7**, 442–451.
87. Westacott, M.J., Farnsworth, N.L., St Clair, J.R., Poffenberger, G., Heintz, A., Ludin, N.W., Hart, N.J., Powers, A.C. and Benninger, R.K.P. (2017) Age-dependent decline in the coordinated (Ca²⁺) and insulin secretory dynamics in Human pancreatic islets. *Diabetes*, **66**, 2436–2445.
88. Henquin, J.-C. (2018) Influence of organ donor attributes and preparation characteristics on the dynamics of insulin secretion in isolated human islets. *Physiol. Rep.*, **6**, e13646.
89. Butler, A., Hoffman, P., Smibert, P., Papalexi, E. and Satija, R. (2018) Integrating single-cell transcriptomic data across different conditions, technologies, and species. *Nat. Biotechnol.*, **36**, 411–420.
90. Luecken, M.D., Büttner, M., Chaichoompu, K., Danese, A., Interlandi, M., Mueller, M.F., Strobl, D.C., Zappia, L., Dugas, M., Colomé-Tatché, M. *et al.* (2022) Benchmarking atlas-level data integration in single-cell genomics. *Nat. Methods*, **19**, 41–50.
91. Aibar, S., González-Blas, C.B., Moerman, T., Wouters, J., Huynh-Thu, V.A., Imrichova, H., Atak, Z.K., Hulselmans, G., Dewaele, M., Rambow, F. *et al.* SCENIC: single-cell regulatory network inference and clustering. *Nat. Methods*, **14**, 1083–1086.
92. Huynh-Thu, V.A., Irrthum, A., Wehenkel, L. and Geurts, P. (2010) Inferring regulatory networks from expression data using tree-based methods. *PLoS One*, **5**, e12776.
93. Young, M.D. and Behjati, S. (2020) SoupX removes ambient RNA contamination from droplet-based single-cell RNA sequencing data. *Gigascience*, **9**, g1aa151.
94. McGinnis, C.S., Murrow, L.M. and Gartner, Z.J. (2019) DoubletFinder: doublet detection in single-cell RNA sequencing data using artificial nearest neighbors. *Cell Syst.*, **8**, 329–337.
95. Cosentino, C., Toivonen, S., Diaz Villamil, E., Atta, M., Ravanat, J.-L., Demine, S., Schiavo, A.A., Pachera, N., Deglasse, J.-P., Jonas, J.-C. *et al.* (2018) Pancreatic β -cell tRNA hypomethylation and fragmentation link TRMT10A deficiency with diabetes. *Nucleic Acids Res.*, **46**, 10302–10318.
96. Lytrivi, M., Senée, V., Salpea, P., Fantuzzi, F., Philippi, A., Abdulkarim, B., Sawatani, T., Marín-Cañas, S., Pachera, N., Degavre, A. *et al.* (2021) DNAJC3 deficiency induces β -cell mitochondrial apoptosis and causes syndromic young-onset diabetes. *Eur. J. Endocrinol.*, **184**, 455–468.
97. Fantuzzi, F., Toivonen, S., Schiavo, A.A., Chae, H., Tariq, M., Sawatani, T., Pachera, N., Cai, Y., Vinci, C., Virgilio, E. *et al.* (2022) In depth functional characterization of human induced pluripotent stem cell-derived beta cells in vitro and in vivo. *Front. Cell Dev. Biol.*, **10**, 967765.
98. De Franco, E., Lytrivi, M., Ibrahim, H., Montaser, H., Wakeling, M.N., Fantuzzi, F., Patel, K., Demarez, C., Cai, Y., Igoillo-Esteve, M. *et al.* (2020) YIPF5 mutations cause neonatal diabetes and microcephaly through endoplasmic reticulum stress. *J. Clin. Invest.*, **130**, 6338–6353.
99. Demine, S., Schiavo, A.A., Marín-Cañas, S., Marchetti, P., Cnop, M. and Eizirik, D.L. (2020) Pro-inflammatory cytokines induce cell death, inflammatory responses, and endoplasmic reticulum stress in human iPSC-derived beta cells. *Stem Cell Res Ther.*, **11**, 7.
100. Kharroubi, I., Ladrrière, L., Cardozo, A.K., Dogusan, Z., Cnop, M. and Eizirik, D.L. (2004) Free fatty acids and cytokines induce pancreatic beta-cell apoptosis by different mechanisms: role of nuclear factor-kappaB and endoplasmic reticulum stress. *Endocrinology*, **145**, 5087–5096.
101. Cunha, D.A., Ladrrière, L., Ortis, F., Igoillo-Esteve, M., Gurzov, E.N., Lupi, R., Marchetti, P., Eizirik, D.L. and Cnop, M. (2009) Glucagon-like peptide-1 agonists protect pancreatic beta-cells from lipotoxic endoplasmic reticulum stress through upregulation of BiP and JunB. *Diabetes*, **58**, 2851–2862.
102. Cunha, D.A., Igoillo-Esteve, M., Gurzov, E.N., Germano, C.M., Naamane, N., Marfour, I., Fukaya, M., Vanderwinden, J.-M., Gysemans, C., Mathieu, C. *et al.* (2012) Death protein 5 and p53-upregulated modulator of apoptosis mediate the endoplasmic reticulum stress-mitochondrial dialog triggering lipotoxic rodent and human β -cell apoptosis. *Diabetes*, **61**, 2763–2775.
103. Cunha, D.A., Cito, M., Carlsson, P.-O., Vanderwinden, J.-M., Molkenin, J.D., Bugliani, M., Marchetti, P., Eizirik, D.L. and Cnop, M. (2016) Thrombospondin 1 protects pancreatic β -cells from lipotoxicity via the PERK-NRF2 pathway. *Cell Death Differ.*, **23**, 1995–2006.
104. Roca-Rivada, A., Marín-Cañas, S., Colli, M.L., Vinci, C., Sawatani, T., Marselli, L., Cnop, M., Marchetti, P. and Eizirik, D.L. (2023) Inhibition of the type 1 diabetes candidate gene PTPN2 aggravates TNF- α -induced human beta cell dysfunction and death. *Diabetologia*, **66**, 1544–1556.
105. Hoorens, A., Van de Castele, M., Klöppel, G. and Pipeleers, D. (1996) Glucose promotes survival of rat pancreatic beta cells by activating synthesis of proteins which suppress a constitutive apoptotic program. *J. Clin. Invest.*, **98**, 1568–1574.
106. Marroqui, L., Masini, M., Merino, B., Grieco, F.A., Millard, I., Dubois, C., Quesada, I., Marchetti, P., Cnop, M. and Eizirik, D.L. (2015) Pancreatic α cells are resistant to metabolic stress-induced apoptosis in type 2 diabetes. *EBioMedicine*, **2**, 378–385.
107. Vanheer, L., Song, J., De Geest, N., Janiszewski, A., Talon, I., Provenzano, C., Oh, T., Chappell, J. and Pasque, V. (2019) Tox4 modulates cell fate reprogramming. *J. Cell Sci.*, **132**, jcs232223.
108. Ceulemans, A., Verhulst, S., Van Haele, M., Govaere, O., Ventura, J.-J., van Grunsven, L.A. and Roskams, T. (2017) RNA-sequencing-based comparative analysis of human hepatic progenitor cells and their niche from alcoholic steatohepatitis livers. *Cell Death. Dis.*, **8**, e3164.
109. Hafemeister, C. and Satija, R. (2019) Normalization and variance stabilization of single-cell RNA-seq data using regularized negative binomial regression. *Genome Biol.*, **20**, 296.
110. Stuart, T., Butler, A., Hoffman, P., Hafemeister, C., Papalexi, E., Mauck, W.M. 3rd, Hao, Y., Stoerckius, M., Smibert, P. and Satija, R. (2019) Comprehensive integration of single-cell data. *Cell*, **177**, 1888–1902.
111. Wierup, N., Svensson, H., Mulder, H. and Sundler, F. (2002) The ghrelin cell: a novel developmentally regulated islet cell in the human pancreas. *Regul. Pept.*, **107**, 63–69.
112. Sande, B.V., Van de Sande, B., Flerin, C., Davie, K., De Waegeneer, M., Hulselmans, G., Aibar, S., Seurinck, R., Saelens, W., Cannoodt, R. *et al.* (2020) A scalable SCENIC workflow for single-cell gene regulatory network analysis. *Nat. Protoc.*, **15**, 2247–2276.
113. Arda, H.E., Tsai, J., Rosli, Y.R., Giresi, P., Bottino, R., Greenleaf, W.J., Chang, H.Y. and Kim, S.K. (2018) A chromatin basis for cell lineage and disease risk in the Human pancreas. *Cell Syst.*, **7**, 310–322.
114. Rai, V., Quang, D.X., Erdos, M.R., Cusanovich, D.A., Daza, R.M., Narisu, N., Zou, L.S., Didion, J.P., Guan, Y., Shendure, J. *et al.* (2020) Single-cell ATAC-seq in human pancreatic islets and deep learning upscaling of rare cells reveals cell-specific type 2 diabetes regulatory signatures. *Mol. Metab.*, **32**, 109–121.
115. Hart, A.W., Mella, S., Mendrychowski, J., van Heyningen, V. and Kleinjan, D.A. (2013) The developmental regulator Pax6 is essential for maintenance of islet cell function in the adult mouse pancreas. *PLoS One*, **8**, e54173.
116. Mosedale, M., Egodage, S., Calma, R.C., Chi, N.-W. and Chessler, S.D. (2012) Neurexin-1 α contributes to insulin-containing secretory granule docking. *J. Biol. Chem.*, **287**, 6350–6361.
117. Hwang, I.-H., Park, J., Kim, J.M., Kim, S.I., Choi, J.-S., Lee, K.-B., Yun, S.H., Lee, M.-G., Park, S.J. and Jang, I.-S. (2016) Tetraspanin-2 promotes glucotoxic apoptosis by regulating the JNK/ β -catenin signaling pathway in human pancreatic β cells. *FASEB J.*, **30**, 3107–3116.
118. Daraio, T., Bombek, L.K., Gosak, M., Valladolid-Acebes, I., Klemen, M.S., Refai, E., Berggren, P.-O., Brismar, K., Rupnik, M.S. and Bark, C. (2017) SNAP-25b-deficiency increases insulin secretion and changes spatiotemporal profile of Ca²⁺-oscillations in β cell networks. *Sci. Rep.*, **7**, 7744.
119. Juan-Mateu, J., Rech, T.H., Villate, O., Lizarraga-Mollinedo, E., Wendt, A., Turatsinze, J.-V., Brondani, L.A., Nardelli, T.R., Nogueira, T.C., Esguerra, J.L.S. *et al.* (2017) Neuron-enriched

- RNA-binding proteins regulate pancreatic beta cell function and survival. *J. Biol. Chem.*, **292**, 3466–3480.
120. Aljaijeji, H., Mukhopadhyay, D., Mohammed, A.K., Dhaiban, S., Hachim, M.Y., Elemam, N.M., Sulaiman, N., Salehi, A. and Taneera, J. (2019) Reduced expression of PLCXD3 associates with disruption of glucose sensing and insulin signaling in pancreatic β -cells. *Front. Endocrinol.*, **10**, 735.
 121. Gierl, M.S., Karoulias, N., Wende, H., Strehle, M. and Birchmeier, C. (2006) The zinc-finger factor Insm1 (IA-1) is essential for the development of pancreatic beta cells and intestinal endocrine cells. *Genes Dev.*, **20**, 2465–2478.
 122. Haumaitre, C., Lenoir, O. and Scharfmann, R. (2008) Histone deacetylase inhibitors modify pancreatic cell fate determination and amplify endocrine progenitors. *Mol. Cell. Biol.*, **28**, 6373–6383.
 123. Nissim, S., Weeks, O., Talbot, J.C., Hedgepeth, J.W., Wucherpfennig, J., Schatzman-Bone, S., Swinburne, I., Cortes, M., Alexa, K., Megason, S. et al. (2016) Iterative use of nuclear receptor Nr5a2 regulates multiple stages of liver and pancreas development. *Dev. Biol.*, **418**, 108–123.
 124. Kropp, P.A., Zhu, X. and Gannon, M. (2019) Regulation of the Pancreatic Exocrine Differentiation Program and morphogenesis by Omeut 1/Hnf6. *Cell. Mol. Gastroenterol. Hepatol.*, **7**, 841–856.
 125. Quilichini, E., Fabre, M., Dirami, T., Stedman, A., De Vas, M., Ozguc, O., Pasek, R.C., Cereghini, S., Morillon, L., Guerra, C. et al. (2019) Pancreatic ductal deletion of Hnf1b disrupts exocrine homeostasis, leads to pancreatitis, and facilitates tumorigenesis. *Cell. Mol. Gastroenterol. Hepatol.*, **8**, 487–511.
 126. Bray, J.K., Elgamil, O.A., Jiang, J., Wright, L.S., Sutaria, D.S., Badawi, M., Borczyk, M.G., Liu, X., Fredenburg, K.M., Campbell-Thompson, M.L. et al. (2020) Loss of RE-1 silencing transcription factor accelerates exocrine damage from pancreatic injury. *Cell Death. Dis.*, **11**, 138.
 127. Eletto, D., Eletto, D., Boyle, S. and Argon, Y. (2016) PDIA6 regulates insulin secretion by selectively inhibiting the RIDD activity of IRE1. *FASEB J.*, **30**, 653–665.
 128. Rorsman, P. and Ashcroft, F.M. (2018) Pancreatic β -cell electrical activity and insulin secretion: of mice and men. *Physiol. Rev.*, **98**, 117–214.
 129. Carrasco, M., Delgado, I., Soria, B., Martín, F. and Rojas, A. (2012) GATA4 and GATA6 control mouse pancreas organogenesis. *J. Clin. Invest.*, **122**, 3504–3515.
 130. Masui, T., Swift, G.H., Deering, T., Shen, C., Coats, W.S., Long, Q., Elsässer, H.-P., Magnuson, M.A. and MacDonald, R.J. (2010) Replacement of Rbpj with Rbpjl in the PTF1 complex controls the final maturation of pancreatic acinar cells. *Gastroenterology*, **139**, 270–280.
 131. Yamashita, J., Ohmoto, M., Yamaguchi, T., Matsumoto, I. and Hirota, J. (2017) Skn-1a/Pou2f3 functions as a master regulator to generate Trpm5-expressing chemosensory cells in mice. *PLoS One*, **12**, e0189340.
 132. Delporte, F.M., Pasque, V., Devos, N., Manfroid, I., Voz, M.L., Motte, P., Biemar, F., Martial, J.A. and Peers, B. (2008) Expression of zebrafish pax6b in pancreas is regulated by two enhancers containing highly conserved cis-elements bound by PDX1, PBX and PREP factors. *BMC Dev. Biol.*, **8**, 53.
 133. Dorrell, C., Schug, J., Lin, C.F., Canaday, P.S., Fox, A.J., Smirnova, O., Bonnah, R., Streeter, P.R., Stoekert, C.J. Jr, Kaestner, K.H. et al. (2011) Transcriptomes of the major human pancreatic cell types. *Diabetologia*, **54**, 2832–2844.
 134. Leung-Theung-Long, S., Roulet, E., Clerc, P., Escricut, C., Marchal-Victorion, S., Ritz-Laser, B., Philippe, J., Pradayrol, L., Seva, C., Fourmy, D. et al. (2005) Essential interaction of egr-1 at an islet-specific response element for basal and gastrin-dependent glucagon gene transactivation in pancreatic α -cells. *J. Biol. Chem.*, **280**, 7976–7984.
 135. Eto, K., Kaur, V. and Thomas, M.K. (2007) Regulation of pancreas duodenum homeobox-1 expression by early growth response-1. *J. Biol. Chem.*, **282**, 5973–5983.
 136. Yu, J.H. and Kim, H. (2012) Role of janus kinase/signal transducers and activators of transcription in the pathogenesis of pancreatitis and pancreatic cancer. *Gut Liver*, **6**, 417–422.
 137. Good, A.L., Cannon, C.E., Haemmerle, M.W., Yang, J., Stanescu, D.E., Doliba, N.M., Birnbaum, M.J. and Stoffers, D.A. (2019) JUND regulates pancreatic β cell survival during metabolic stress. *Mol. Metab.*, **25**, 95–106.
 138. Wang, K., Cui, Y., Lin, P., Yao, Z. and Sun, Y. (2021) JunD regulates pancreatic β -cells function by altering lipid accumulation. *Front. Endocrinol.*, **12**, 689845.
 139. Kaestner, K.H., Powers, A.C., Naji, A., Consortium, H. and Atkinson, M.A. (2019) NIH initiative to improve understanding of the Pancreas, islet, and autoimmunity in type 1 diabetes: the Human Pancreas Analysis Program (HPAP). *Diabetes*, **68**, 1394–1402.
 140. Shin, S., Asano, T., Yao, Y., Zhang, R., Claret, F.-X., Korc, M., Sabapathy, K., Menter, D.G., Abbruzzese, J.L. and Reddy, S.A.G. (2009) Activator protein-1 has an essential role in pancreatic cancer cells and is regulated by a novel Akt-mediated mechanism. *Mol. Cancer Res.*, **7**, 745–754.
 141. Recio-Boiles, A., Ilmer, M., Robyn Rhea, P., Kettlun, C., Heinemann, M.L., Ruetering, J., Vykoukal, J. and Alt, E. (2016) JNK pathway inhibition selectively primes pancreatic cancer stem cells to TRAIL-induced apoptosis without affecting the physiology of normal tissue resident stem cells. *OncoTargets Ther.*, **7**, 9890–9906.
 142. Miyazaki, S., Taniguchi, H., Moritoh, Y., Tashiro, F., Yamamoto, T., Yamato, E., Ikegami, H., Ozato, K. and Miyazaki, J.-I. (2010) Nuclear hormone retinoid X receptor (RXR) negatively regulates the glucose-stimulated insulin secretion of pancreatic β -cells. *Diabetes*, **59**, 2854–2861.
 143. Mastracci, T.L. and Sussel, L. (2012) The endocrine pancreas: insights into development, differentiation, and diabetes. *Wiley Interdiscip. Rev.: Dev. Biol.*, **1**, 609–628.
 144. Cantile, M., Franco, R., Tschan, A., Baumhoer, D., Zlobec, I., Schiavo, G., Forte, I., Bihl, M., Liguori, G., Botti, G. et al. (2009) HOX D13 expression across 79 tumor tissue types. *Int. J. Cancer*, **125**, 1532–1541.
 145. Sato, F., Kawamura, H., Wu, Y., Sato, H., Jin, D., Bhawal, U.K., Kawamoto, T., Fujimoto, K., Noshiro, M., Seino, H. et al. (2012) The basic helix-loop-helix transcription factor DEC2 inhibits TGF- β -induced tumor progression in human pancreatic cancer BxPC-3 cells. *Int. J. Mol. Med.*, **30**, 495–501.
 146. Schuijers, J., Junker, J.P., Mokry, M., Hatzis, P., Koo, B.-K., Sasselli, V., van der Flier, L.G., Cuppen, E., van Oudenaarden, A. and Clevers, H. (2015) Ascl2 acts as an R-spondin/wnt-responsive switch to control stemness in intestinal crypts. *Cell Stem Cell*, **16**, 158–170.
 147. Vethe, H., Ghila, L., Berle, M., Hoareau, L., Haaland, Ø.A., Scholz, H., Paulo, J.A., Chera, S. and Ræder, H. (2019) The effect of wnt pathway modulators on Human iPSC-derived pancreatic beta cell maturation. *Front. Endocrinol.*, **10**, 293.
 148. Sharon, N., Vanderhooft, J., Straubhaar, J., Mueller, J., Chawla, R., Zhou, Q., Engquist, E.N., Trapnell, C., Gifford, D.K. and Melton, D.A. (2019) Wnt signaling separates the progenitor and endocrine compartments during pancreas development. *Cell Rep.*, **27**, 2281–2291.
 149. Arystarkhova, E., Liu, Y.B., Salazar, C., Stanojevic, V., Clifford, R.J., Kaplan, J.H., Kidder, G.M. and Swadner, K.J. (2013) Hyperplasia of pancreatic beta cells and improved glucose tolerance in mice deficient in the FXFD2 subunit of Na,K-ATPase. *J. Biol. Chem.*, **288**, 7077–7085.
 150. Vierra, N.C., Dadi, P.K., Jeong, I., Dickerson, M., Powell, D.R. and Jacobson, D.A. (2015) Type 2 diabetes-associated K⁺ channel TALK-1 modulates β -cell electrical excitability, second-phase insulin secretion, and glucose homeostasis. *Diabetes*, **64**, 3818–3828.
 151. Flamez, D., Roland, I., Berton, A., Kutlu, B., Dufrane, D., Beckers, M.C., De Waele, E., Rooman, I., Bouwens, L., Clark, A. et al. (2010) A genomic-based approach identifies FXFD2 domain containing ion transport regulator 2 (FXFD2) as a pancreatic beta cell-specific biomarker. *Diabetologia*, **53**, 1372–1383.
 152. Baranek, C., Sock, E. and Wegner, M. (2005) The POU protein Oct-6 is a nucleocytoplasmic shuttling protein. *Nucleic Acids Res.*, **33**, 6277–6286.
 153. Zhu, R., Yang, Y., Tian, Y., Bai, J., Zhang, X., Li, X., Peng, Z., He, Y., Chen, L., Pan, Q. et al. (2012) Ascl2 knockdown results in tumor growth arrest by miRNA-302b-related inhibition of colon cancer progenitor cells. *PLoS One*, **7**, e32170.
 154. Xu, H., Zhao, X.-L., Liu, X., Hu, X.-G., Fu, W.-J., Li, Q., Wang, Y., Ping, Y.-F., Zhang, X., Bian, X.-W. et al. (2017) Elevated ASCL2 expression in breast cancer is associated with the poor prognosis of patients. *Am. J. Cancer Res.*, **7**, 955–961.

155. Hamaguchi, H., Fujimoto, K., Kawamoto, T., Noshiro, M., Maemura, K., Takeda, N., Nagai, R., Furukawa, M., Honma, S., Honma, K.-I. *et al.* (2004) Expression of the gene for Dec2, a basic helix-loop-helix transcription factor, is regulated by a molecular clock system. *Biochem. J.*, **382**, 43–50.
156. Meissner, H.P. and Atwater, I.J. (1976) The kinetics of electrical activity of beta cells in response to a 'square wave' stimulation with glucose or glibenclamide. *Horm. Metab. Res.*, **8**, 11–16.
157. Braun, M., Ramracheya, R., Bengtsson, M., Zhang, Q., Karanaukaite, J., Partridge, C., Johnson, P.R. and Rorsman, P. (2008) Voltage-gated ion channels in human pancreatic beta-cells: electrophysiological characterization and role in insulin secretion. *Diabetes*, **57**, 1618–1628.
158. Regazzi, R., Wollheim, C.B., Lang, J., Theler, J.M., Rossetto, O., Montecucco, C., Sadoul, K., Weller, U., Palmer, M. and Thorens, B. (1995) VAMP-2 and cellubrevin are expressed in pancreatic beta-cells and are essential for Ca(2+)-but not for GTP gamma S-induced insulin secretion. *EMBO J.*, **14**, 2723–2730.
159. Refai, E., Dekki, N., Yang, S.-N., Imreh, G., Cabrera, O., Yu, L., Yang, G., Norgren, S., Rössner, S.M., Inverardi, L. *et al.* (2005) Transthyretin constitutes a functional component in pancreatic β -cell stimulus-secretion coupling. *Proc. Natl. Acad. Sci. U.S.A.*, **102**, 17020–17025.
160. Stefan, Y., Meda, P., Neufeld, M. and Orci, L. (1987) Stimulation of insulin secretion reveals heterogeneity of pancreatic B cells in vivo. *J. Clin. Invest.*, **80**, 175–183.
161. Sakikubo, M., Furuyama, K., Horiguchi, M., Hosokawa, S., Aoyama, Y., Tsuboi, K., Goto, T., Hirata, K., Masui, T., Dor, Y. *et al.* (2018) Ptf1a inactivation in adult pancreatic acinar cells causes apoptosis through activation of the endoplasmic reticulum stress pathway. *Sci. Rep.*, **8**, 15812.
162. Tosti, L., Hang, Y., Debnath, O., Tiesmeyer, S., Trefzer, T., Steiger, K., Ten, F.W., Lukassen, S., Ballke, S., Kühl, A.A. *et al.* (2021) Single-nucleus and In situ RNA-sequencing reveal cell topographies in the Human pancreas. *Gastroenterology*, **160**, 1330–1344.
163. Backx, E., Wauters, E., Baldan, J., Van Bulck, M., Michiels, E., Heremans, Y., De Paep, D.L., Kurokawa, M., Goyama, S., Bouwens, L. *et al.* (2021) MECOM permits pancreatic acinar cell dedifferentiation avoiding cell death under stress conditions. *Cell Death Differ.*, **28**, 2601–2615.
164. Weng, C.-C., Hsieh, M.-J., Wu, C.-C., Lin, Y.-C., Shan, Y.-S., Hung, W.-C., Chen, L.-T. and Cheng, K.-H. (2019) Loss of the transcriptional repressor TGIF1 results in enhanced Kras-driven development of pancreatic cancer. *Mol. Cancer*, **18**, 96.
165. Parajuli, P., Singh, P., Wang, Z., Li, L., Eragamreddi, S., Ozkan, S., Ferrigno, O., Prunier, C., Razaque, M.S., Xu, K. *et al.* (2019) TGIF1 functions as a tumor suppressor in pancreatic ductal adenocarcinoma. *EMBO J.*, **38**, e101067.
166. Cordá-Esteban, N., Naumann, H., Ruzittu, S., Mah, N., Pongrac, I.M., Cozzitorto, C., Hommel, A., Andrade-Navarro, M.A., Bonifacio, E. and Spagnoli, F.M. (2017) Stepwise reprogramming of liver cells to a pancreas progenitor state by the transcriptional regulator Tgfi2. *Nat. Commun.*, **8**, 14127.
167. Gomez, D.L., O'Driscoll, M., Sheets, T.P., Hruban, R.H., Oberholzer, J., McGarrigle, J.J. and Shambloot, M.J. (2015) Neurogenin 3 expressing cells in the Human exocrine pancreas have the capacity for endocrine cell fate. *PLoS One*, **10**, e0133862.
168. Matsumoto, K., Mizoshita, T., Tsukamoto, T., Ogasawara, N., Hirata, A., Shimizu, Y., Haneda, M., Yamao, K. and Tatematsu, M. (2004) Cdx2 expression in pancreatic tumors: relationship with prognosis of invasive ductal carcinomas. *Oncol. Rep.*, **12**, 1239–1243.
169. Coleman, J.D., Thompson, J.T., Smith, R.W. 3rd, Prokopczyk, B. and Vanden Heuvel, J.P. (2013) Role of peroxisome proliferator-activated receptor $\beta/8$ and B-cell lymphoma-6 in regulation of genes involved in metastasis and migration in pancreatic cancer cells. *PPAR Res*, **2013**, 121956.
170. Leung-Theung-Long, S., Roulet, E., Clerc, P., Escrieut, C., Marchal-Victorin, S., Ritz-Laser, B., Philippe, J., Pradayrol, L., Seva, C., Fourmy, D. *et al.* (2005) Essential interaction of Egr-1 at an islet-specific response element for basal and gastrin-dependent glucagon gene transactivation in pancreatic alpha-cells. *J. Biol. Chem.*, **280**, 7976–7984.
171. Cheng, K., Ho, K., Stokes, R., Scott, C., Lau, S.M., Hawthorne, W.J., O'Connell, P.J., Loudovaris, T., Kay, T.W., Kulkarni, R.N. *et al.* (2010) Hypoxia-inducible factor-1alpha regulates beta cell function in mouse and human islets. *J. Clin. Invest.*, **120**, 2171–2183.
172. Swisa, A., Glaser, B. and Dor, Y. (2017) Metabolic stress and compromised identity of pancreatic beta cells. *Front. Genet.*, **8**, 21.
173. Guo, S., Dai, C., Guo, M., Taylor, B., Harmon, J.S., Sander, M., Robertson, R.P., Powers, A.C. and Stein, R. (2013) Inactivation of specific β cell transcription factors in type 2 diabetes. *J. Clin. Invest.*, **123**, 3305–3316.
174. Weedon, M.N., Cebola, I., Patch, A.-M., Flanagan, S.E., De Franco, E., Caswell, R., Rodriguez-Segui, S.A., Shaw-Smith, C., Cho, C.H.-H., Allen, H.L. *et al.* (2014) Recessive mutations in a distal PTF1A enhancer cause isolated pancreatic agenesis. *Nat. Genet.*, **46**, 61–64.
175. Nicolino, M., Claiborn, K.C., Senée, V., Boland, A., Stoffers, D.A. and Julier, C. (2010) A novel hypomorphic PDX1 mutation responsible for permanent neonatal diabetes with subclinical exocrine deficiency. *Diabetes*, **59**, 733–740.
176. Patel, K.A., Kettunen, J., Laakso, M., Stančáková, A., Laver, T.W., Colclough, K., Johnson, M.B., Abramowicz, M., Groop, L., Miettinen, P.J. *et al.* (2017) Heterozygous RFX6 protein truncating variants are associated with MODY with reduced penetrance. *Nat. Commun.*, **8**, 888.
177. Cnop, M., Abdulkarim, B., Bottu, G., Cunha, D.A., Igoillo-Esteve, M., Masini, M., Turatsinze, J.-V., Griebel, T., Villate, O., Santin, I. *et al.* (2014) RNA sequencing identifies dysregulation of the human pancreatic islet transcriptome by the saturated fatty acid palmitate. *Diabetes*, **63**, 1978–1993.
178. Cnop, M., Toivonen, S., Igoillo-Esteve, M. and Salpea, P. (2017) Endoplasmic reticulum stress and eIF2 α phosphorylation: the Achilles heel of pancreatic β cells. *Mol. Metab.*, **6**, 1024–1039.
179. Eizirik, D.L., Pasquali, L. and Cnop, M. (2020) Pancreatic β -cells in type 1 and type 2 diabetes mellitus: different pathways to failure. *Nat. Rev. Endocrinol.*, **16**, 349–362.
180. Boden, G., Chen, X. and Polansky, M. (1999) Disruption of circadian insulin secretion is associated with reduced glucose uptake in first-degree relatives of patients with type 2 diabetes. *Diabetes*, **48**, 2182–2188.
181. Pappa, K.I., Gazouli, M., Anastasiou, E., Iliodromiti, Z., Antsaklis, A. and Anagnou, N.P. (2013) The major circadian pacemaker ARNT-like protein-1 (BMAL1) is associated with susceptibility to gestational diabetes mellitus. *Diabetes Res. Clin. Pract.*, **99**, 151–157.
182. Alvarez-Dominguez, J.R., Donaghey, J., Rasouli, N., Kenty, J.H.R., Helman, A., Charlton, J., Straubhaar, J.R., Meissner, A. and Melton, D.A. (2020) Circadian entrainment triggers maturation of Human In vitro islets. *Cell Stem Cell*, **26**, 108–122.
183. Langmesser, S., Tallone, T., Bordon, A., Rusconi, S. and Albrecht, U. (2008) Interaction of circadian clock proteins PER2 and CRY with BMAL1 and CLOCK. *BMC Mol. Biol.*, **9**, 41.
184. Fujimoto, K., Hamaguchi, H., Hashiba, T., Nakamura, T., Kawamoto, T., Sato, F., Noshiro, M., Bhawal, U.K., Suardita, K. and Kato, Y. (2007) Transcriptional repression by the basic helix-loop-helix protein Dec2: multiple mechanisms through E-box elements. *Int. J. Mol. Med.*, **19**, 925–932.
185. He, Y., Jones, C.R., Fujiki, N., Xu, Y., Guo, B., Holder, J.L. Jr, Rossner, M.J., Nishino, S. and Fu, Y.-H. (2009) The transcriptional repressor DEC2 regulates sleep length in mammals. *Science*, **325**, 866–870.
186. Gale, J.E., Cox, H.I., Qian, J., Block, G.D., Colwell, C.S. and Matveyenko, A.V. (2011) Disruption of circadian rhythms accelerates development of diabetes through pancreatic beta-cell loss and dysfunction. *J. Biol. Rhythms*, **26**, 423–433.
187. Wu, Y., Tian, T., Wu, Y., Yang, Y., Zhang, Y. and Qin, X. (2021) Systematic studies of the circadian clock genes impact on temperature compensation and cell proliferation using CRISPR tools. *Biology*, **10**, 1204.
188. Oster, H., Yasui, A., van der Horst, G.T.J. and Albrecht, U. (2002) Disruption of mCry2 restores circadian rhythmicity in mPer2 mutant mice. *Genes Dev.*, **16**, 2633–2638.
189. Oster, H., Baeriswyl, S., Van Der Horst, G.T.J. and Albrecht, U. (2003) Loss of circadian rhythmicity in aging mPer1-/-mCry2-/- mutant mice. *Genes Dev.*, **17**, 1366–1379.
190. Hogenesch, J.B. and Herzog, E.D. (2011) Intracellular and intercellular processes determine robustness of the circadian clock. *FEBS Lett.*, **585**, 1427–1434.

191. Xu, Y., Zhang, T., Zhou, Q., Hu, M., Qi, Y., Xue, Y., Nie, Y., Wang, L., Bao, Z. and Shi, W. (2023) A single-cell transcriptome atlas profiles early organogenesis in human embryos. *Nat. Cell Biol.*, **25**, 604–615.
192. Pagliuca, F.W., Millman, J.R., Gürtler, M., Segel, M., Van Dervort, A., Ryu, J.H., Peterson, Q.P., Greiner, D. and Melton, D.A. (2014) Generation of functional human pancreatic β cells in vitro. *Cell*, **159**, 428–439.
193. Nostro, M.C., Sarangi, F., Yang, C., Holland, A., Elefanty, A.G., Stanley, E.G., Greiner, D.L. and Keller, G. (2015) Efficient generation of NKX6-1+ pancreatic progenitors from multiple human pluripotent stem cell lines. *Stem Cell Rep.*, **4**, 591–604.
194. Russ, H.A., Parent, A.V., Ringler, J.J., Hennings, T.G., Nair, G.G., Shveygert, M., Guo, T., Puri, S., Haataja, L., Cirulli, V. et al. (2015) Controlled induction of human pancreatic progenitors produces functional beta-like cells in vitro. *EMBO J.*, **34**, 1759–1772.
195. Baeyens, L., Lemper, M., Staels, W., De Groef, S., De Leu, N., Heremans, Y., German, M.S. and Heimberg, H. (2018) (Re)generating Human beta cells: status, pitfalls, and perspectives. *Physiol. Rev.*, **98**, 1143–1167.
196. Hoang, C.Q., Hale, M.A., Azevedo-Pouly, A.C., Elsässer, H.P., Deering, T.G., Willet, S.G., Pan, F.C., Magnuson, M.A., Wright, C.V.E., Swift, G.H. et al. (2016) Transcriptional maintenance of pancreatic acinar identity, differentiation, and homeostasis by PTF1A. *Mol. Cell Biol.*, **36**, 3033–3047.
197. Brunton, H., Caligiuri, G., Cunningham, R., Upstill-Goddard, R., Bailey, U.-M., Garner, I.M., Nourse, C., Dreyer, S., Jones, M., Moran-Jones, K. et al. (2020) HNF4A and GATA6 loss reveals therapeutically actionable subtypes in pancreatic cancer. *Cell Rep.*, **31**, 107625.
198. Ahlqvist, E., Storm, P., Käräjämäki, A., Martinell, M., Dorkhan, M., Carlsson, A., Vikman, P., Prasad, R.B., Aly, D.M., Almgren, P. et al. (2018) Novel subgroups of adult-onset diabetes and their association with outcomes: a data-driven cluster analysis of six variables. *Lancet Diabetes Endocrinol.*, **6**, 361–369.
199. Chen, S. and Mar, J.C. (2018) Evaluating methods of inferring gene regulatory networks highlights their lack of performance for single cell gene expression data. *BMC Bioinf.*, **19**, 232.
200. Olbrot, M., Rud, J., Moss, L.G. and Sharma, A. (2002) Identification of β -cell-specific insulin gene transcription factor RIPE3b1 as mammalian MafA. *Proc. Natl. Acad. Sci. U.S.A.*, **99**, 6737–6742.
201. Krentz, N.A.J., van Hoof, D., Li, Z., Watanabe, A., Tang, M., Nian, C., German, M.S. and Lynn, F.C. (2017) Phosphorylation of NEUROG3 links endocrine differentiation to the cell cycle in pancreatic progenitors. *Dev. Cell*, **41**, 129–142.
202. Mastracci, T.L., Wilcox, C.L., Arnes, L., Panea, C., Golden, J.A., May, C.L. and Sussel, L. (2011) Nkx2.2 and Arx genetically interact to regulate pancreatic endocrine cell development and endocrine hormone expression. *Dev. Biol.*, **359**, 1–11.
203. Butte, A.J., Tamayo, P., Slonim, D., Golub, T.R. and Kohane, I.S. (2000) Discovering functional relationships between RNA expression and chemotherapeutic susceptibility using relevance networks. *Proc. Natl. Acad. Sci. U.S.A.*, **97**, 12182–12186.
204. Bevacqua, R.J., Dai, X., Lam, J.Y., Gu, X., Friedlander, M.S.H., Tellez, K., Miguel-Escalada, I., Bonàs-Guarch, S., Atla, G., Zhao, W. et al. (2021) CRISPR-based genome editing in primary human pancreatic islet cells. *Nat. Commun.*, **12**, 2397.
205. Hopcroft, D.W., Mason, D.R. and Scott, R.S. (1985) Structure-function relationships in pancreatic islets: support for intraislet modulation of insulin secretion. *Endocrinology*, **117**, 2073–2080.